Mechanical behavior of polyurea nanocomposites doped with nanoparticles

Émilien Billaudeau


RESEARCH REPORT

Mechanical behavior of polyurea nanocomposites doped with nanoparticles

Emilien Billaudeau
Ecole Centrale Lyon

September 2010

Raimondo Betti, Haim Waisman
Columbia University in the city of New York (USA)

Monssef Drissi-Habti
Laboratoire des Ponts et Chaussées de Nantes (France)

Michelle Salvia
Ecole Centrale Lyon (France)

Blank page

Acknowledgments

My most earnest acknowledgment must go to my advisors from Columbia University[1], professors Betti and Waisman who have been instrumental in ensuring my integration in the Civil Engineering department. I also thank them to have given me scientific and financial support to perform my study.

My internship would not have been possible without the matchless help I got from Dr. Monssef Drissi-Habti from the LCPC[2] who connected me with this laboratory and helped me in my research. This training period is conducted within the framework of the collaboration going on between LCPC and Columbia University.

My gratitude also stretches to my second French advisor, Pr. Michelle Salvia from the ECL[3]. Her experience in material science and particularly in composites was really helpful.

Mr. Adrian Brugger and Dr. Liming Li from the Carleton laboratory (Department of Civil Engineering at Columbia University) are greatly acknowledged for their assistance with the material manufacturing and the tension tests.

I would also like to thank Oya Okman for her help with the Scanning Electron Microscope and for her training session in order to give me access.

Last but not least, i would like to express my gratitude to Dr. Jorgen Bergstrom[4] for his extra support he gave me on the computational modeling.

[1](New York, USA)
[2]Laboratoire Central des Ponts et Chaussées (Nantes, France)
[3]Ecole Centrale (Lyon, France)
[4]MIT Ph.D., Veryst Engineering (Boston, USA)

Abstract

Recently, carbon nanotubes and graphene nanoplatelets have attracted both academic and industrial interest because of their capacity to produce a dramatic improvement in properties at very low filler content. In this work, we focused on experimental studies and computational modeling of polymer nanocomposites intended for passive protection of civil structures. The material considered in this study consisted of a polyurea matrix enhanced by different quantities of nanoparticles. Different renforts and matrixes have been used to fabricate nanoparticles polymer nanocomposites by a range of methods. Several tensile tests were performed to evaluate and characterize the behavior of the studied materials in order to choose the appropriate manufacturing protocol and the suitable enhancement. Furthermore, a finite elements model was achieved The main goal of this study was to achieve a parametric determination of the tested materials in order to find a general model.

The manufacturing protocol study had led to an ultrasonic dispersion of the nanoparticles instead of a mechanical stirring. Degrading the properties of the initial material, the mechanical mixing method does not disaggregate the nanoparticles, which is an important factor in the nanoreinforcement.

The results indicate that an arbitrary amount of carbon nanotubes and graphene nanoplatelets may result in suboptimal performance and more specifically 0.5% in weight of carbon nanotubes and 2% in weight of graphene nanoplatelets yield the best mechanical performance in each nanocomposite family. However, comparing these two optimums, the graphene nanoplatelets doped material leads to the best performance.

Keywords

Nanomaterials; carbon nanotubes; graphene nanoplatelets; polymer matrix; composite material; polyurea; finite elements; hyperelastic modeling.

Abbreviations

CNTs, carbon nanotubes; MWCNTs, multi-wall carbon nanotubes; CVD, chemical vapor deposition; GNPs, graphene nanoplatelets; SEM, scanning electron microscope; THF, tetrahydrofuran.

Résumé

Récemment, les nanotubes de carbone ainsi que les nanoplaquettes de graphène ont attiré à la fois universitaires et industriels en raison de leur capacité à apporter une amélioration spectaculaire des propriétés du composite. Au cours de cette étude, nous nous sommes concentrés sur des études expérimentales et informatiques des nanocomposites à base de polymères destinés à la protection passive des structures de génie civil. Le matériau considéré dans cette étude était constitué d'une matrice polyuréthane renforcée par différentes quantités de nanoparticules. Suivant différentes méthodes, différents renforts et matrices ont été utilisées pour la fabrication des nanocomposites. Plusieurs essais de traction ont été réalisés pour évaluer et caractériser le comportement des matériaux étudiés afin de choisir le protocole de fabrication approprié. En outre, un modèle éléments finis a été développé afin de parvenir à une détermination des paramètres relatifs aux matériaux testés dans le but de trouver un modèle général.

L'étude du protocole de fabrication a conduit à une dispersion des nanoparticules par ultrasons plutôt qu'une agitation mécanique. Dégradants les propriétés de la matrice, la méthode de brassage mécanique ne répartit pas les nanoparticules, ce qui est un facteur important dans la nanorenforcement.

Les résultats de cette étude indiquent qu'une quantité précise de nanotubes de carbone ou de nanoplaquettes de graphène pourrait entraîner une performance optimale. En effet, 0,5 % de nanotubes de carbone et 2 % de nanoplaquettes de graphène permettent d'obtenir les meilleurs performances mécaniques. Toutefois, comparant ces deux optimums, les nanoplaquettes de graphène donnent les meilleures performances.

Contents

List of Figures

List of Tables

1 Introduction

Protection of civil infrastructure from environmental and aging deterioration and other extreme conditions is a key concern in any country and particularly in the United States[12]. In many urban cities, counties and states, the infrastructure suffers from corrosion, deterioration of structural elements due to climate and environmental changes, damage induced by wind or earthquake excitations or by man-made action, aging of materials and many more.

These issues require continuous monitoring, repairs and the strengthening and replacement of damaged components. All of these actions require significant resource allocation for maintenance. The development of new technologies and new materials offers an innovative route to solve some of the problems that currently afflict our infrastructural system. Recently, the production and use of nanoparticles has become a major research theme worldwide[5]. Many applications of these nanoparticles rely on their incorporation into a host matrix to form the so called nanocomposite[6]. The term "nanocomposite" is usually used to describe multiphase solid materials where at least one of the phases is in orders of nanometers. This project consists in the nanoenhancement study in order to find a suitable manufacturing protocol and an optimum of the enhancement amount for the studied nanocomposites.

[5]Bibliography work in appendix (French document)
[6]The bibliography section will introduce these new materials and their properties

2 Literature review

Introducing the context of the study, this literature review describes the enhancement interest in polymer materials. Presenting several functions and properties of the materials involved in the composite and nanocomposite structure, this section highlights some theories on these complex materials.

2.1 Elastomer presentation

2.1.1 Mechanical properties

Elastomer is a polymer with the property of viscoelasticity[7]. What makes elastomers special is the fact that they can be stretched to many times their original length, and they can bounce back into their original shape without plastic deformation. The schematic drawing in figure 1 shows the elastomer structure. The behavior is due to the overlap of molecular chains (curved lines) and the cross-links (Black circles). Under stress, the molecules are forced to line up in the direction in which the rubber is being pulled. The covalent cross-linkages (energetic bond) ensure that the elastomer will return to its initial morphology when the stress is removed. As a result of this extreme elasticity, elastomers can reversely extend from 5-700% (depending on the material).

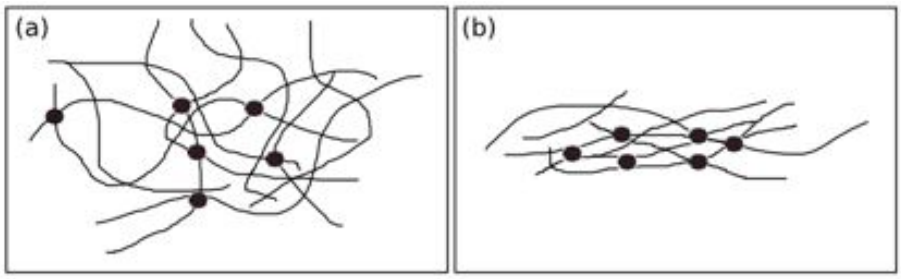

Figure 1: (a) Schematic drawing of unstressed elastomer; (b) Same elastomer under stress

Figure 2 shows SEM pictures [1] of the deformed elastomer during uni-axial tensile test (pictures at strains of 1.7, 5.5 and 7.4). As previously introduced and according to the SEM pictures (b,c,d), the distortion of the elastomer structure is highlighted. Because of its large deformation and its low stress, the curve (a) shows the hyperelastic behavior of the elastomers.

Because of the high viscoelasticity, the mechanical properties of the elastomers are strongly rate dependent. As presented in the article [13], the failure stress increases and the failure strain decreases with the strain rate. To be coherent, elastomer studies require standards tests and modeling to get comparable results [7]. These methods will be presented in the following section and in the appendix *Strain rate in the rubber materials*.

Temperature effect is also an important parameter in the rubber studies. Called the glass transition, this parameter exhibits an ultimate work temperature for the studied material. Glass transition is the temperature above which a polymer becomes soft and pliable, and below which it becomes hard and glassy.

[7]Property that exhibit both viscous and elastic characteristics when undergoing deformation

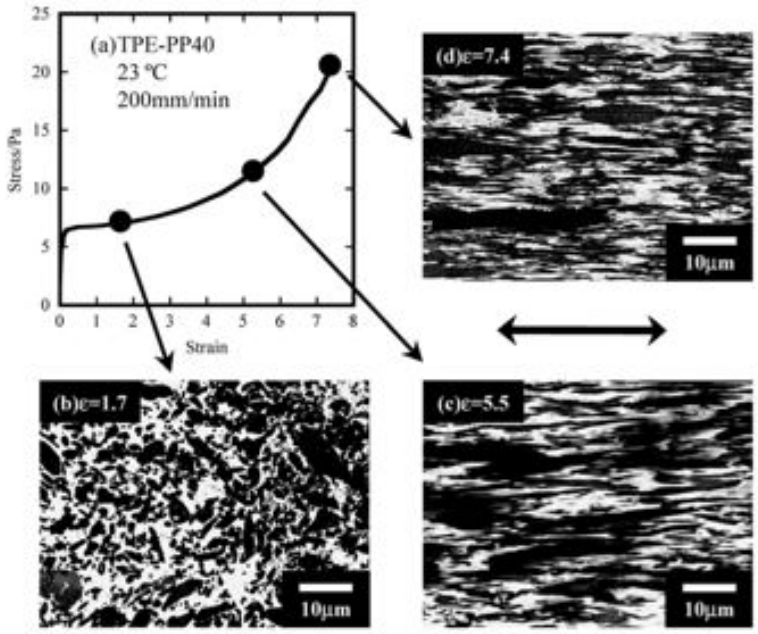

Figure 2: SEM pictures of elastomer (TPE-PP40). (a) Load-elongation curves. The SEM pictures of the material drawn at (b) strain = 1.7, (c) strain = 5.5, (d) strain = 7.4 [1]

2.1.2 Polyurea

Polyurea is a fast reacting bi-component polymer system that contains 70% of amine. The first component is isocyanate, a -NCO group, which is the curative part, while the other one is a resin blend component. The reaction between the two components yields a urea linkage that makes the polymer solid.

The resulting polyurea is an elastomer that is usually sprayed under high pressure/temperature to produce a thick, strong and seamless waterproof coating with incredible abrasion, corrosion and chemical resistance. Due to these characteristics, this kind of material seems attractive in the civil infrastructure application.

2.2 Enhancement interest

2.2.1 An example, the tire

Tires are the most important and least understood parts of the vehicle. Everything concerned with driving, moving, starting, stopping involves tires. Because of their functions, tires have several main constraints, which are:

1. Abrasion, wear and tear resistance
2. Carry vehicle's weight

3. Transmit forces

4. Withstand shocks

In order to get a part meeting the above requirements, a sophisticated material structure is needed. As shown in figure 3, a tire has a complex structure where each material has a unique role.

First, an elastomer covering is needed to absorb the shocks (hyperelastic material)), resisting against abrasion and insuring a control of the vehicle due to the material's viscosity (forces transmission).

Second, an enhancement is required to ensure a mechanical resistance. In this example, the reinforcement is made of steel cable layers following different directions in order to get a strong structure in the high strength areas.

Figure 3: Cut tire *(Ref : http://www.aviation-fr.info/avion/pneus.php)*

2.2.2 Composite families

Tires are among the most famous example for composites based on elastomer and fiber enhancement. Founded on similar general meanings, several kinds of composites are now developed[8]:

1. Short or long fibers reinforcement

2. Metal, concrete or polymer matrix

3. Stratified, sandwich or tissue composites

4. Macro, micro or nano enhancement

[8]These materials are not presented in this literature review, the aim is to introduce the composite interest

Nano-reinforcement is currently under consideration. The three sections below present these new composites with their interests. This review introduces severals nano-enhancements and the nanocomposite's expected properties.

2.3 Carbon nanotubes

Discovered in 1991 by Pr. Iijima, a carbon nanotube (CNT) is a cylindrical molecule with outer diameter of 4-30 nm and a length of up to 1 microns [6]. The fashion of this molecule is due to its impressive properties in several domains (mechanical [17, 14], electrical [10, 5] or optical [5]).

2.3.1 High performances

This unique structure presented in figure 4 displays these properties. The perfect arrangement of carbon atoms, linked by covalent bonds[9], limits the structural defects causing high mechanical strength. Table 1 compares the mechanical properties of the CNTs with its competitors. As shown in this table, the CNTs have a mechanical strength greater than that of Steel or Kevlar and a density lower than that of Aluminum.

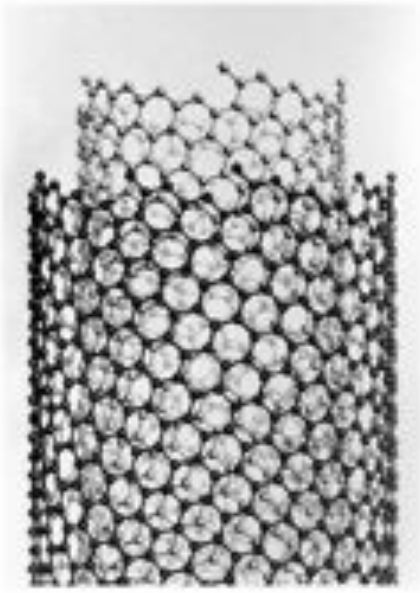

Figure 4: Multi-wall carbon nanotubes (MWNTs) [6]

[9]Energetic bound

Properties	CNTs	Competitors
Young Modulus	1 TPa	Steel : 200 GPa
Tensile Strength	45 GPa	Kevlar : 3.5 GPa
Density	1.3 g/cm3	Aluminum : 2.7 g/cm3

Table 1: CNTs properties

2.3.2 Growing methods

Since their discovery, several growing techniques were developed to make these new molecules. The first two growth methods of carbon nanotubes were based on the graphite[10] evaporation using an arc discharge or a laser ablation in an oven (Temperature about 1200 degrees Celsius). At controlled temperature and pressure, the volatile molecules condensed on a substrate forming carbon nanotubes. These two methods, costly in energy, were replaced by a chemical method called CVD[11]. This synthesis (illustrated in figure 5) is achieved taking a carbon species in the gas phase (methane or carbon monoxide, for example) and using an energy source (oven) to "crack" the molecules. These species then diffuse down to a substrate (quartz boat in the example) in order to form the CNTs. Since CVD is a simple and relatively cheap technique, it might be the most promising method for large-scale production of CNTs.

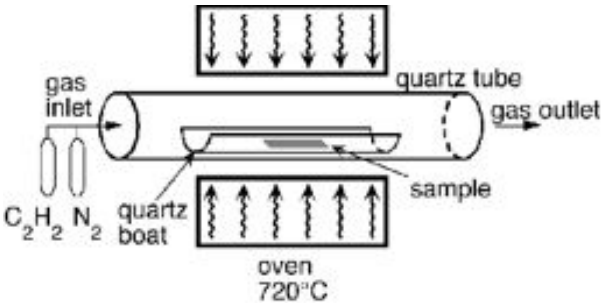

Figure 5: CVD method *(Ref : http://ipn2.epfl.ch/CHBU/NTproduction1.htm)*

2.4 Graphene Nanoplatelets

2.4.1 Presentation and properties

Graphene is the basic structural unit of some carbon allotropes [4, 8], including graphite, carbon nanotubes and fullerenes. Graphene can be prepared using similar methods as CNTs. Graphene is a single layer of carbon atoms packed densely in a honeycomb crystal lattice (figure 6). Along with its unique structure, graphene

[10]The most stable carbon configuration
[11]Chemical Vapor Deposition

possesses a range of unusual properties like mechanical stiffness, strength and electrical and thermal conductivity. Figure 7 shows graphene nanoplatelets which are composed by numbers of graphene sheets. These particles have an average thickness of approximately 6-8 nanometers and a typical surface area of 150 m^2/g.

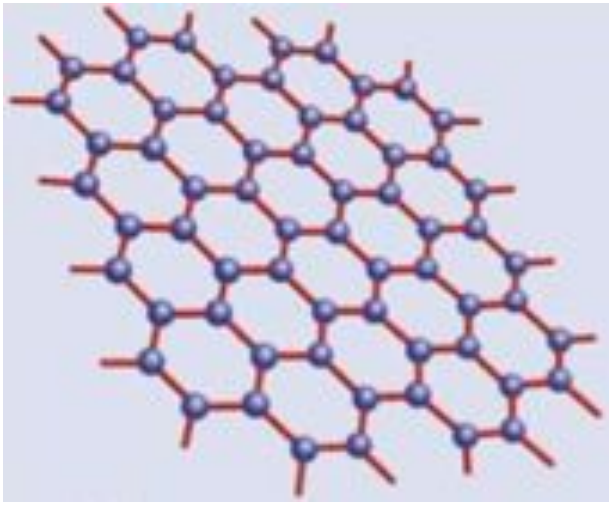

Figure 6: Graphene sheet

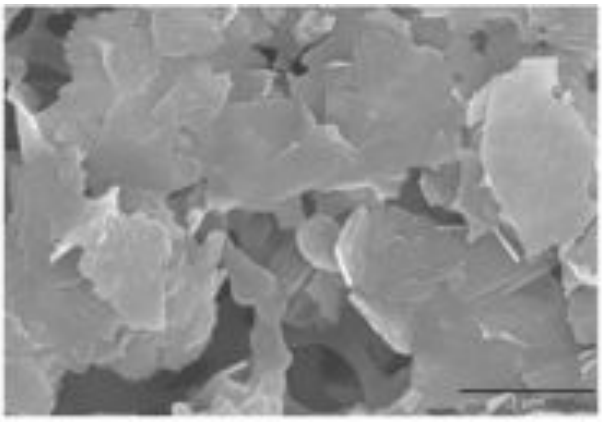

Figure 7: SEM picture of graphene nanoplatelets *(Ref : http://www.xgscience.com/products.html)*

2.4.2 Comparison with the CNTs

Table 2 shows the GNP mechanical properties. Comparing these properties with that of the CNT, it is shown that the behavior is similar, the main difference between these particles is their shapes.

Properties	CNTs	GNPs
Young Modulus	1 TPa	1 TPa
Tensile Strength	45 GPa	10-20 GPa
Density	1.3 g/cm3	2.0 g/cm3

Table 2: Comparison between CNTs and GNPs mechanical properties

2.5 Nanocomposites

As presented in the above two sections, due to their impressive properties, CNTs and GNPs are envisaged to be the ideal reinforcement for polymer composites, especially for the enhancement of the mechanical properties [9]. However, while adding nanoparticles in a polymer matrix can enhance its performance, according to some theories, it can also degrade the initial behavior of the matrix. As presented below, composite properties are strongly influenced by the matrix enhancement interface, the fiber's behavior and their dispersion.

2.5.1 Parameters influencing the nanocomposite behavior

Fiber's behavior

Due to the nanoparticles ability to deform prior to break (hyper-elastic behavior), they give greater hardness than the carbon or glass fiber based composites which have a lower toughness because of the brittleness of the fibers.

Interface matrix/renforts

According to the article [19], a strong interface between the matrix and the fibers makes a composite with high stiffness and strength. A better interfacial adhesion can enhance composite transverse properties or flexural properties. The large interfacial areas are due to the high aspect ratio[12] of CNTs and GNPs, which creates the matrix/renfort stress transfer.

Enhancement dispersion

The nanoparticles dispersion [11, 15] in the polymer matrix is the key parameter to get the expected behavior. Picture 8 on page 20 shows the CNTs network needed to improve the polymer behavior. Several dispersion methods are presented in the appendix called *Which solvent for the nanoparticles dispersion*. The main aim is to obtain a homogeneous solution in order to get a spread out reinforcement. A bad dispersion causes an enhancement in the nanoparticle's aggregates, allowing for several areas poor in CNTs or GNPs.

[12]Length/Diameter

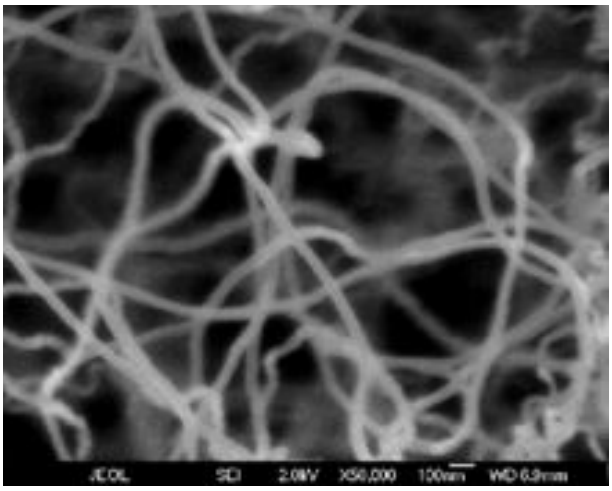

Figure 8: CNTs network for polymer-based nanocomposites *(Ref : http://www.nano-lab.com/)*

2.5.2 Process review

Since the nanoparticles discovery, some manufacturing processes [20, 8] have been developed. the most effective processes are presented below.

Solution mixing and film casting

Solution mixing is based on a solvent system in which the polymer or pre-polymer is solublized and CNTs or GNPs are allowed to swell. Stirring CNTs or GNPs in a solvent is efficient due to the low viscosity of the solution. In this way, the particles motion is easier and the dispersion is more homogenous. These nanoparticles can be dispersed easily in a suitable solvent, such as water, acetone, chloroform, tetrahydrofuran (THF), dimethylformamide (DMF) or toluene. Nevertheless, this method requires the use of a solvent which is expensive and need to be evaporated before the polymerization.

Melt mixing (extrusion, injection molding)

Without any solvent, the particles mix with the polymer matrix in the molten state. On one hand, by overcoming the need of the solvent, this method is cheaper than the first one, but on the other hand, the dispersion is worse (due to the high viscosity).

In-situ polymerization

In this manufacturing method, the nanoparticles are first swollen within the liquid monomer. A suitable initiator is then diffused and polymerization is initiated either by heat or radiation. This process has the advantage to stir the renfort in a low viscosity liquid without the need of a solvent. Due to its low price and its efficiency, this method is currently the most used in the nanocomposite manufacturing.

3 Materials and methods

This section presents the methods used to conduct the research. The subsections that follow explain the materials used to perform the study; the several protocols found to make the nanocomposites; the tests completed to describe the nanocomposite's behavior and the hyperelastic modeling used to predict the general performance of this kind of composite.

3.1 Manufacturing and experimental tests

3.1.1 Materials manufacturing

Materials used

The Multi-Walled Carbon nanotubes (CNTs) used in this study were purchased from Sigma Aldrich and were synthetized by Catalitic Chemical Vapor Deposition (CVD).

The Graphene Naoplatelets (GNPs) xGnP-M-15 were purchased from XG Science, Inc. and were also synthetized by CVD.

The Polyurea used in this study was ordered from ITW Futura Coatings as Aqualine 300 and from ITW Devcon as Flexane 80 liquid 15800 (equivalent to the Aqualine 300).

Tetrahydrofuran (THF) anhydrous was purchased from Sigma Aldrich. This is an organic solvent that is used to disperse CNTs in the polymer matrix. Ethanol and distilled water were also used as solvent in the nanoparticles dispersion.

The nanocomposite specimens have been prepared by adding different quantities in weight percentage [wt%] of nanoparticles (CNTs or GSs) as follows:

1. Polyurea
2. Polyurea + solvent + 0.1 wt% (CNTs or GNPs)
3. Polyurea + solvent + 0.5 wt% (CNTs or GNPs)
4. Polyurea + solvent + 1 wt% (CNTs or GNPs)
5. Polyurea + solvent + 1.5 wt% (CNTs or GNPs)
6. Polyurea + solvent + 2 wt% (CNTs or GNPs)
7. Polyurea + solvent + 2.5 wt% (CNTs or GNPs)
8. Polyurea + solvent + 5 wt% (CNTs or GNPs)

Table 3 indicates the needed quantities to manufacture the different nanocomposites (around 30 g per sample).

One of the main goals is to evaluate which of the above mentioned nanocomposites yields the best overall mechanical performance.

Instrumentation

The nanoparticles dispersion was performed mixing the solution with a rotative helix *IKA RW 20 digital*.

CNTs or GNPs [wt%]	0	0.1	0.5	1	1.5	2	2.5	5
CNTs or GNPs [g]	0	0.06	0.3	0.6	0.9	1.2	1.5	3
Resin part [g]	46.2	46.1	46.0	45.7	45.5	45.3	45.0	43.9
Curative part [g]	13.8	13.8	13.7	13.7	13.6	13.5	13.5	13.1
Solvent [ml]	0	50	50	50	50	50	50	50
total[13] [g]	60	60	60	60	60	60	60	60

Table 3: Nanocomposite compositions

Another way to disperse these nanoparticles was the use of a probe sonicator *hielscher UP50H* and a ultrasonic bath *L&R ultrasonic Guantrex 90*.

A centrifuge *Sorvall LEGEND X1, Thermo Scientific* was also used to validate the nanoparticles dispersion in the solvent.

The polymerization acceleration and the solvent evaporation (if needed) was performed in a Vacuum oven *Shel Lab VPX9-2* according to the Polyurea instructions.

An aluminium mold was manufactured to produce specimens with constant dimensions.

Protocols

To produce the nanocomposite specimens (nanoparticles + matrix), different quantities of enhancement have been added (as mentioned above). The objective is to determine the optimal structure for this material.

Due to the available materials (matrix composed of resin and hardener) the mixing solution protocol (presented in the literature review) had to been chosen to make the suitable nanocomposites. The first method used to produce these materials is explained below.

- To make the nanocomposites, nanoparticles were first dissolved in 50 ml of THF and stirred for 30 minutes using the rotating helix (2000 rpm).
- Then the curative part was added to the mix and stirred for another 30 minutes until the mixture became homogeneous.
- Finally, the resin part was added and the new mixture was mixed for an additional 5 minutes to get a homogeneous mix.
- The enhanced polymer was then poured into 5mm thick paper-boxes and stored for 4 days at controlled temperature/humidity to let the polymerization process cure until a hard nanocomposite material was created. Once cured, this nanocomposite was subdivided into stripes according to the standard ASTM D-412 to obtain the specimens suitable for the mechanical tests.

With the results found, the method had to be changed. In fact, the main point in the nanocomposite research was the nanoparticles dispersion in the matrix. An efficient method that needed an ultrasonic processor was used to get better results [11]. We also used an aluminum mold to get better precision in the specimen's dimensions. The improved protocol follows.

- Like the first protocol, the nanoparticles were first dissolved in 50 ml of solvent (chose from a study presented in the appendix) and stirred for 45 minutes using the probe sonicator (Frequency : 30 kHz, Amplitude : 100 %, Cycle : 0.9[14]). It is known that the ultra-sons are efficient for the dispersion, but it is also known that the ultra-sons damage the CNTs (after 1 hour the CNTs are 2 micrometer shorter). Balanced between a good dispersion (needed for the nanocomposite enhancement) and good nanoparticle's geometry (also useful to have a better load transfer in the matrix), this step is one of the most important in the manufacturing.

- This solution was heated in order to evaporate the solvent and to keep only the nanoparticles unagglomerated (very thin powder). At controlled temperature (around the solvent boiling temperature), the solution was heated until the complete evaporation of the solvent (controlled by weighing the solution).

- This powder and the resin were stirred for 5 minutes using the rotation helix and then another 15 minutes in the ultrasonic bath.

- Before the casting step, the curative part was added in the solution and stirred for 5 minutes (around 500 rpm, to avoid creating bubbles). This solution was then hand mixed using a spatula to remove as many bubbles as possible. To facilitate the release[15] after the polymerization process cure (10 hours in the mold), the mold was covered with a wax layer.

- 7 days of waiting were necessary to be sure of the properties[16] and to obtain the specimens suitable for the mechanical tests.

3.1.2 Experimental tests

Instrumentation

Tensile tests were controlled in displacement. According to the ASTM D-412: "Standard test methods for vulcanized rubber and thermoplastic elastomers - Tension" [7], tension tests were performed using an *Instron 30K* Universal Testing Machine with a strain rate of 50.8 mm/min (2.00 inch/min). Tested specimen section was measured with a numerical caliper, in order to determine the engineering stress in the material using the tensile machine load measure.

[14] 0.9 second on / 0.1 second off
[15] Polyurea adhesion on the aluminum
[16] Hardness : 80% after 2 days, 100% after 7 days

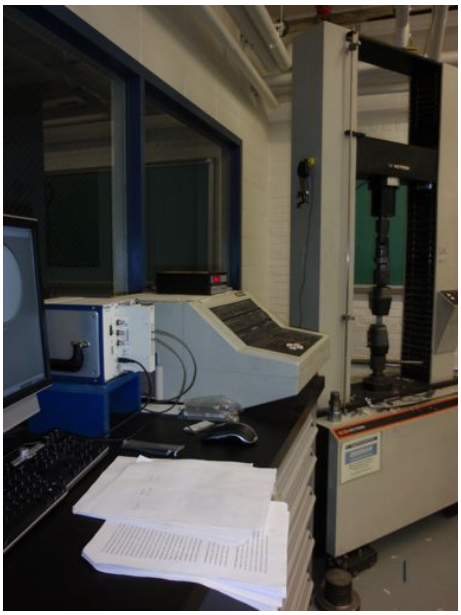

Figure 9: Facilities in the laboratory

Alignment procedure of the tensile machine

Tensile testing requires a precise mods alignment in order to get an accurate result. Stresses that inadvertently occur due to misalignment between the applied force and the specimen axes during tensile forces can affect the test results. Before a uni-axial tensile test, the user has to make certain of the machine alignment to get a free stress sample (in the tested area). Then using a steel sheet fixed in the machine (replacing the sample), the mods were then screwed respecting the alignment controlled by the steel sheet. Figure 10 shows the tensile test and particularly the mods alignment.

3.2 Material modeling

Some constitutive models are able to describe the mechanical behavior of rubber materials. Based on quasi-static[17] calculation, these models allow the material description using materials parameters (for simple behavior materials, the modeling is frequently determined manually). Due to the long strain behavior of the elastomer, the parameters definition is not trivial. In fact, the broad investigation domain does not allow the determination of a law for the whole range of deformation. Therefore, due to the complex theory used to model the rubber material (hyperelastic material with a strain rate dependence), the model research evaluated the material model using experimental data found in the previous part and using an optimization software to model the material.

[17] A quasi-static process often ensures that the system will go through a sequence of states that are infinitesimally close to equilibrium (so the system remains in quasi-static equilibrium), in which case the process is typically reversible.

(a) (b)

Figure 10: Uni-axial tensile test: (a) Strain = 0; (b) Strain = 400%

The main goal of this study is to achieve a parametric determination for several nanocomposites, in order to find a general model.

3.2.1 Modeling using an MCalibration optimization

What is MCalibration?

Developed by Jorgen Bergstrom[18], MCalibration is a material evaluation software using experimental data. Due to its many material models [2] and their algorithms, this program is suitable for our modeling. Some sophisticated models are available in this software. The respective algorithms[19] are based on the comparison between the model curve and experimental data curve, in order to reduce this gap by changing the model parameters.

The way to use MCalibration

The first modeling step is based on the experimental data treatment in order to use them in the MCalibration optimization. To get an efficient material evaluation, the experimental stress/strain curves had to be smoothed. Figure 11 presents the Matlab smoothing. The appendix *Matlab smoothing program* shows the program.

Figure 12 presents the experimental data used as the MCalibration input file.

[18]MIT Ph.D., Veryst Engineering

[19]By choice, the algorithms are not presented in this report, they are introduced in the article [2]

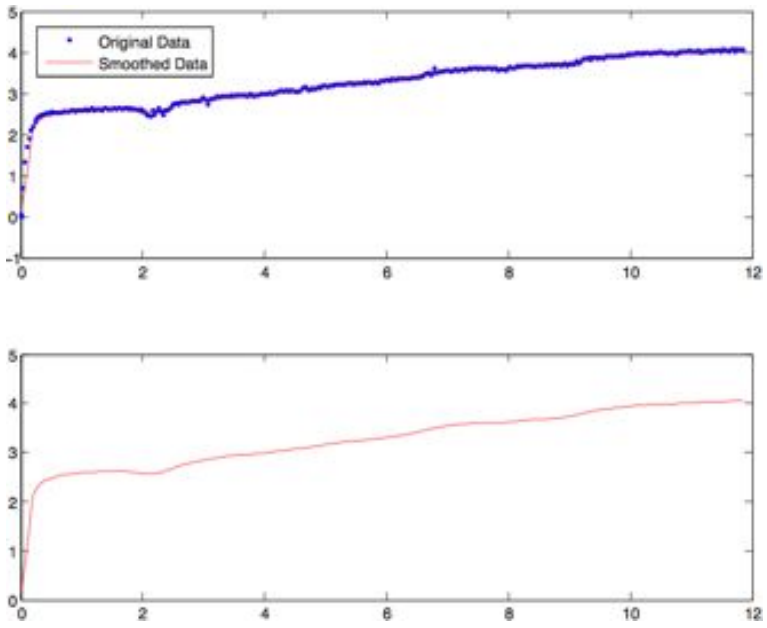

Figure 11: Matlab smoothing (1 wt% (CNTs))

Due to the strain rate[20] of the studied material, the time for each increment needs to be quantified in order to evaluate the model. This time has been arbitrarily determined because of the impossibility of the tensile machine to measure it. The way to compensate[21] this arbitrary time is described in the next paragraph, *Interaction between MCalibration and Abaqus*.

To generate the optimization, some program lines are needed. Figure 13 shows this MCalibration program [3].

- The second *loadcase* tells the experimental data used for the material evaluation, their meaning (engineering or true values) and the kind of test used to get these results.
- The material model chosen is presented in the *MaterialModel* section. In the program presented in figure 13 on page 29, the studied material model is the Ogden model. The following parameters are evaluated using an algorithm developed for this model [2, 3].
- The first *loadcase*, called virtual experiment, is needed to evaluate the Abaqus results using the parameters found by the MCalibration evaluation. In that case, a cycle was tested (load until 200% of engineering strain, unload until 0 MPa of engineering stress). In this section the strain rate was needed to evaluate the material behavior (the appendix presents the influence of the strain

[20] dependence on the solicitation speed
[21] To get comparable results as the experimental tests

Time	Strain (%)	Engineering Stress (MPa)
0	0	0
2.0000000E-01	2.3923997E-02	1.1496050E+00
3.0000000E-01	4.3453997E-02	1.7136469E+00
4.0000000E-01	6.6889130E-02	2.0987950E+00
5.0000000E-01	9.0081130E-02	2.3913391E+00
6.0000000E-01	1.0981133E-01	2.5744422E+00
7.0000000E-01	1.3304666E-01	2.7449176E+00
8.0000000E-01	1.5697133E-01	2.8564632E+00
9.0000000E-01	1.7601266E-01	2.9406486E+00
1.0000000E+00	1.9969266E-01	2.9869505E+00
1.1000000E+00	2.2312866E-01	3.0058922E+00
1.2000000E+00	2.4241400E-01	3.0079969E+00
1.3000000E+00	2.6633866E-01	3.0353571E+00
1.4000000E+00	2.8977400E-01	3.0500895E+00
1.5000000E+00	3.1296600E-01	3.0458803E+00
1.6000000E+00	3.3225200E-01	3.0690312E+00
1.7000000E+00	3.5642000E-01	3.0795544E+00
1.8000000E+00	3.7936733E-01	3.0963915E+00
1.9000000E+00	3.9865333E-01	3.0858683E+00
2.0000000E+00	4.2257733E-01	3.0879730E+00
2.1000000E+00	4.4576933E-01	3.1111239E+00
2.2000000E+00	4.6529933E-01	3.0600000E+00
2.3000000E+00	4.8922133E-01	3.0800000E+00
2.4000000E+00	5.1241466E-01	3.0800000E+00
2.5000000E+00	5.3218866E-01	3.1000000E+00
2.6000000E+00	5.5513666E-01	3.1300000E+00
2.7000000E+00	5.7857200E-01	3.1153332E+00
2.8000000E+00	5.9785800E-01	3.1384842E+00
2.9000000E+00	6.2129400E-01	3.1889954E+00
3.0000000E+00	6.4497400E-01	3.2037278E+00
3.1000000E+00	6.6474800E-01	3.2331927E+00

Figure 12: Experimental data used for the MCalibration optimization

rate and the required method to get results comparable with the experimental data).

Figure 14 compares the material model found by the optimization (SegmentTest (prediction)) with the experimental data (SegmentTest (experimental)) and the virtual experiment (prediction) curve in order to validate the material evaluation. This curve shows a good match between the calculated model and the input data.

3.2.2 Abaqus model definition

Interaction between MCalibration and Abaqus

Using an Abaqus input file written by MCalibration (figure 15), the Abaqus material definition is workable. The Appendix *Interaction between MCalibration and Abaqus* presents the method to fill the estimated parameters in the Abaqus material definition tool. This file informs on the model. The first two parameter lines indicate which model was calculated, while the following lines explain the evaluated parameters.

Boundary conditions and calculation steps

The step following the material definition is to determine the Abaqus model [16] needed to estimate the behavior of the evaluated material. This step consists of the definition of the geometry, its boundary conditions and the calculation options required on the Abaqus model.

```
Loadcase
      name = virtual_experiment
      loadingMode = uniaxial
      orientation = global
      strainType = engineering
      stressType = engineering

control = segments
      Segment
            run eng_strain_rate = 0.2
            until eng_strain = 1.5
            dt0 = 0.01
            dtMin = 1e-05
            dtMax = 0.01
      Segment
            run eng_strain_rate = -0.2
            until eng_stress = 0
            dt0 = 0.01
            dtMin = 1e-05
            dtMax = 0.01

predicted_line_color = brown
predicted_line_width = 3

LoadCase
      name = SegmentTest
      fileName = 1.txt
      loadingMode = uniaxial
      strainType = engineering
      stressType = engineering

Material_Model = Ogden
# ParameterName    Value          opt      minVal      maxVal
      mu1          1.55454         1          -           -
      alpha1       0.360655        2          -           -
      D1           0.01            0          -           -
      mu2          0.258767       11          -           -
      alpha2       1.91837        12          -           -
      D2           0.01            0          -           -
```

Figure 13: MCalibration program (material model optimization)

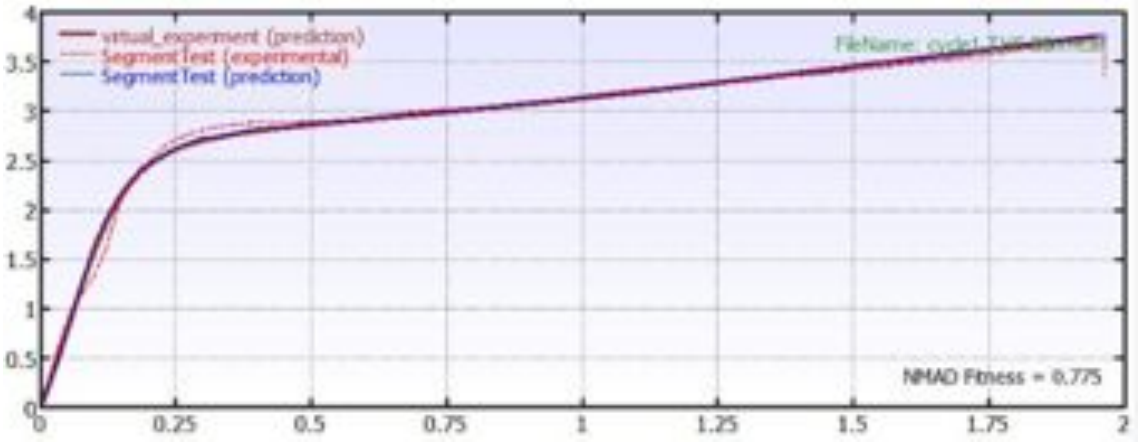

Figure 14: MCalibration optimization result, Engineering stress (MPa) / Engineering strain

```
*Material, name=umat
*User Material, constants=25
** Calibrated using MCalibration
** Units: [length]=millimeter, [force]=Newton, [time]=seconds, [temperature]=Kelvin
** Material Model: Bergstrom-Boyce
** Calibration file name: C:/Program Files (x86)/PolyUMod/Nanocomposite modeling/Mode
**..:....1....:....2....:....3....:....4....:....5....:....6....:....7....:....8
**      MM,       ODE,       JAC,      ERRM,    TWOD_S,      VERB,     VTIME,     VELEM,
         4,         0,         0,         0,         0,         1,         0,         0,
**    VINT,    ORIENT,         -,         -,       GMU,    GKAPPA,     FAILT,     FAILV,
         0,         0,         0,         0,         1,       500,         0,         0,
**      mu,   lambdaL,     kappa,         s,        xi,         C,   tauBase,         m,
   1.06437,   9.99998,   8.75207,    7.5037,  0.999817,  -2.98915,    2.1873,     3.26,
** tauCut
 0.280163
*Depvar
13
*Density
1e-09
```

Figure 15: Abaqus input file (MCalibration exported data)

To get a fast calculation, the cubic part is limited in elements. In fact, a material model needs only simple geometry with at least one element. In this case, the part is subdivided into 200 elements to get a more generalized model (suitable for complex parts modeling).

The boundary conditions used in this model have been chosen to simulate an uni-axial tensile test. Figure 16 presents these boundary conditions.

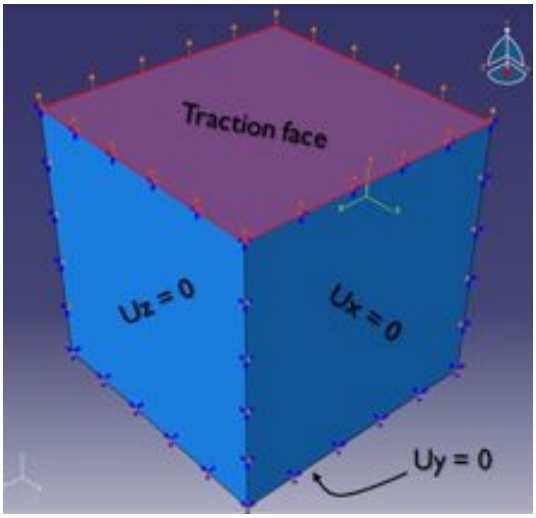

Figure 16: Boundary conditions in Abaqus

According to the tensile machine used in the experimental test, the loading step was controlled in displacement. 500 increments were used during calculation in order to get an accurate and smooth stress/strain curve. The following step is the strain rate determination (rates used in the Abaqus modeling). In order to compensate the arbitrary time used in the MCalibration estimation, the loading time had to be changed[22] to get comparable results between the experimental data and the Abaqus model.

3.2.3 Data treatment

$$\sigma_{engineering} = \left(\frac{1stNodeCoordonate_{t=0}}{1stNodeCoordonate_t} \right)^2 * \sigma_{true} \quad (1)$$

To validate the found model, a data treatment is needed to compare the model results with the experimental data. As presented in the experimental subsection, the engineering stress is the only stress value measured by the tensile machine (the

[22]For example : MCalibration input data loading time = time of the Abaqus loading step

section variation of the sample is not taken in consideration) while the Abaqus calculated stress is the true stress (the section variation is a key parameter for this stress determination), which is the load divided by the true section's part. The formula 1 is used to evaluate the engineering stress using the true stress and a node coordinate (used to estimate the deformed section and to cancel its role in the true stress calculation). This formula was used to determine the engineering stress at each increment.

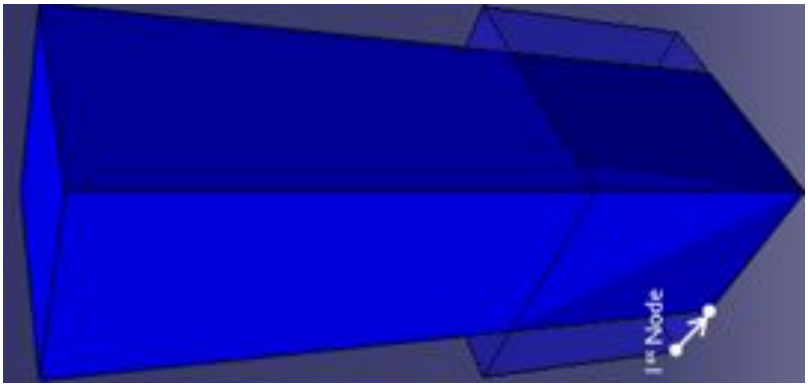

Figure 17: Sample deformation in the Abaqus calculation (1^{st} node coordinate)

4 Results and discussion

This section presents the found results, following the methods presented above. Several nanocomposites were made and tested in the purpose of the behavior prediction and enhancement optimum[23] research. To perform this study, the samples were tested with the tensile machine. Then a fractography analysis followed in order to investigate the reasons of the noticed behavior. This section also presents the model determination and the path to find a general model for the tested materials.

[23] type of enhancement and the amount in the matrix and their amount in the matrix

4.1 Experimental tests

4.1.1 SEM visualization

Scanning Electron Microscope (SEM) images were recorded using a *Hitachi S-4700*. To estimate the needed magnification in order to watch the nanoparticles in the polyurea matrix, we started the SEM visualization using pure CNT and GNP powders glued on carbon stickers. Due to the SEM vacuum chamber, the sample preparation is a key point in this method. It is necessary to ensure the sticking of the nanoparticles (a carbon sheet sticker was used to glue the powders), so that the microscope is not damaged.

Visualizing such particles is a tough task, so a good SEM knowledge is required to get clear pictures [18]. Figure 18 presents the pictures found using the microscope. Due to the different size[24] of the nanoparticles, the magnification needed to visualize these materials oscillates between x25000 for the CNTs and x700 for the GNPs.

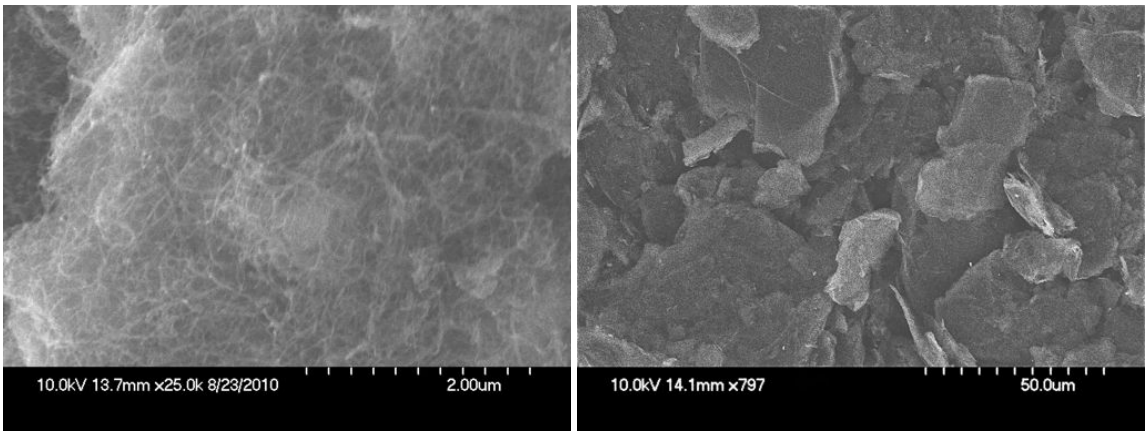

(a) (b)

Figure 18: Nanoparticles visualization: (a) CNTs (Magnification x25000); (b) GNPs (Magnification x787)

4.1.2 First protocol results, CNT enhancement

Mechanical behavior

Figure 19 represents the stress/strain curves for several reinforcement amounts (the crosses symbolize the break of the samples). As shown in these curves, the behavior of the nanocomposites made by following the first protocol is worse than the pure polyurea matrix. In fact, adding nanoreinforcements in a matrix with a mechanical stirring seems to deteriorate the initial material. The result found is therefore inconsistent with the theory presented in the first section. In order to analyse this inconsistency, a microstructure study of the samples is required. The

[24]Introduced in the previous section

following paragraph presents this study and the conclusions reached as a result of it.

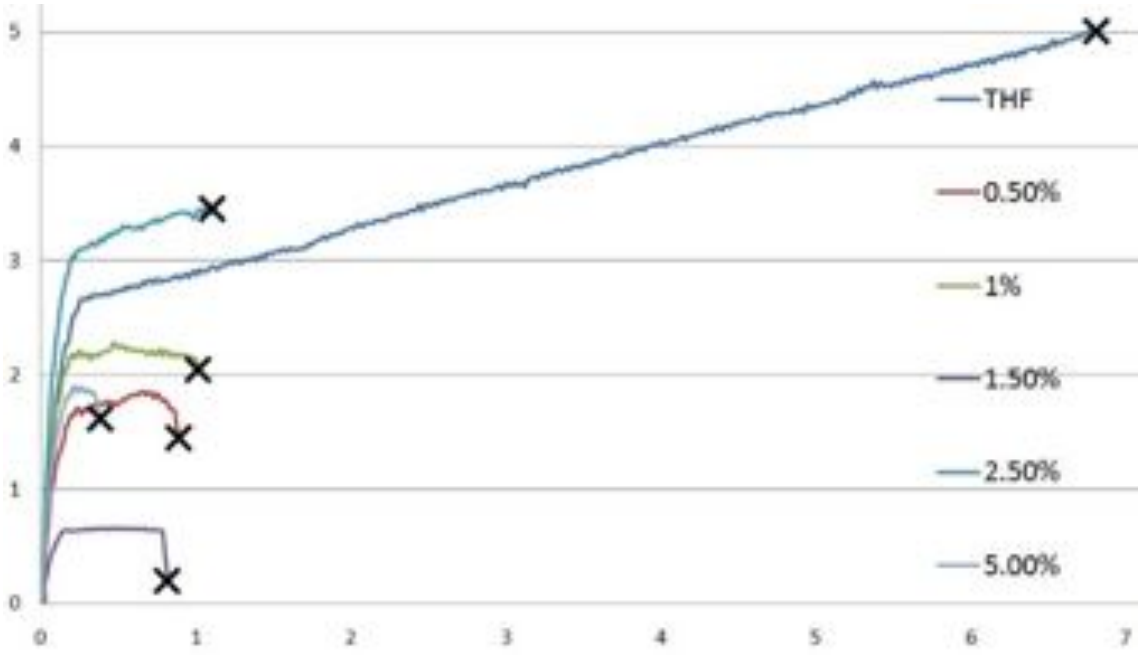

Figure 19: 1^{st} protocol results, Engineering stress (MPa) / Engineering strain

Fractographic analysis

Figure 20 represents the crack sections for the naked matrix (a) and the polyurea matrix enhanced by 1 wt% of CNTs (b). These macro-pictures show the effect of the CNT's dispersion in the matrix. In fact, the nanocomposite is more porous than the pure polyurea because of the bad CNT's dispersion forming agglomerates in the structure. In this case, the agglomerates of CNTs are equivalent to defects, giving a brittle material. These pictures are also useful to show the solvent (THF) effect. In fact, a vacuum area is present in the nanocomposite crack section. This bubble is responsible for the crack propagation during the tensile test. The voids in the matrix are due to the evaporation of the solvent after the polymerization process. In order to avoid this phenomena, solvent evaporation must be made before the polymerization.

These points are also confirmed by microscopic analysis of the nanocomposite samples.

- As shown in fractography 20 (c), the enhancement bound seems weak because of the the height difference between the CNTs aggregate[25] and the matrix. In fact, this visualization conveys the impression of a crack bypass around the aggregate, concluding a low wetting[26] of the reinforcement.

[25]figure 20 (d) shows the aggregate structure, confirming the presence of CNTs
[26]bound capacity of the reinforcement based on the surface tension theory [19]

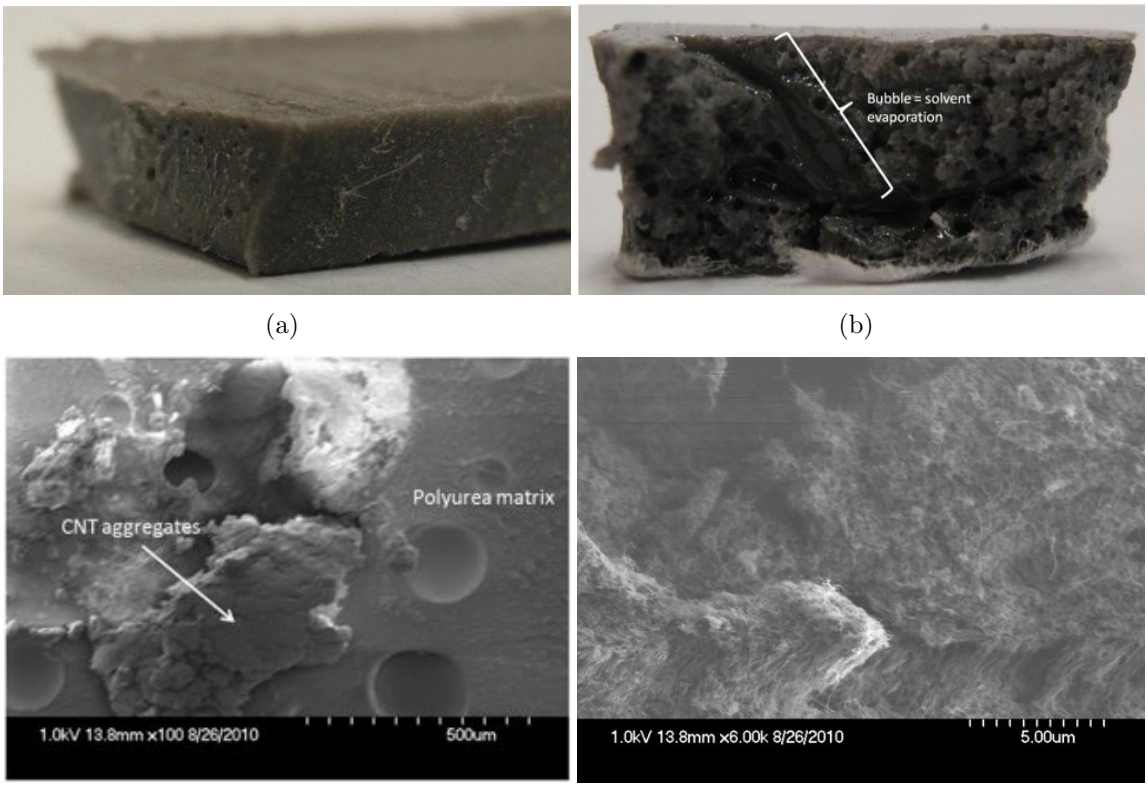

(a) (b)

(c) (d)

Figure 20: First protocol samples: (a) Aqualine 300 picture; (b) Aqualine 300 + THF + 1 wt% of CNTs picture; (c) Aqualine 300 + THF + 1 wt% of CNTs SEM picture (Magnification x100); (d) Aqualine 300 + THF + 1 wt% of CNTs SEM picture (Magnification x6000)

- Otherwise, the bubble in the matrix assumes the solvent evaporation or a fast mechanical stirring. In all cases, this problem degrades the mechanical behavior of the material.

4.1.3 Second protocol results, CNT enhancement

Analyzing the results found by using the first protocol, the manufacturing method had to be modified. Presented as the second protocol in the subsection 3.3.1, the results are from tests on materials produced by this method. In this way, this section highlights the nanoparticle's dispersion effect on the nanocomposite behavior.

Mechanical behavior

From figure 21, it is noteworthy to highlight the mechanical behavior of the CNT-doped nanocomposite using the second manufacturing protocol. As shown in this graphic, it seems evident that the nanotubes are capable of a large strain reinforcement, increasing the mechanical properties of the material.

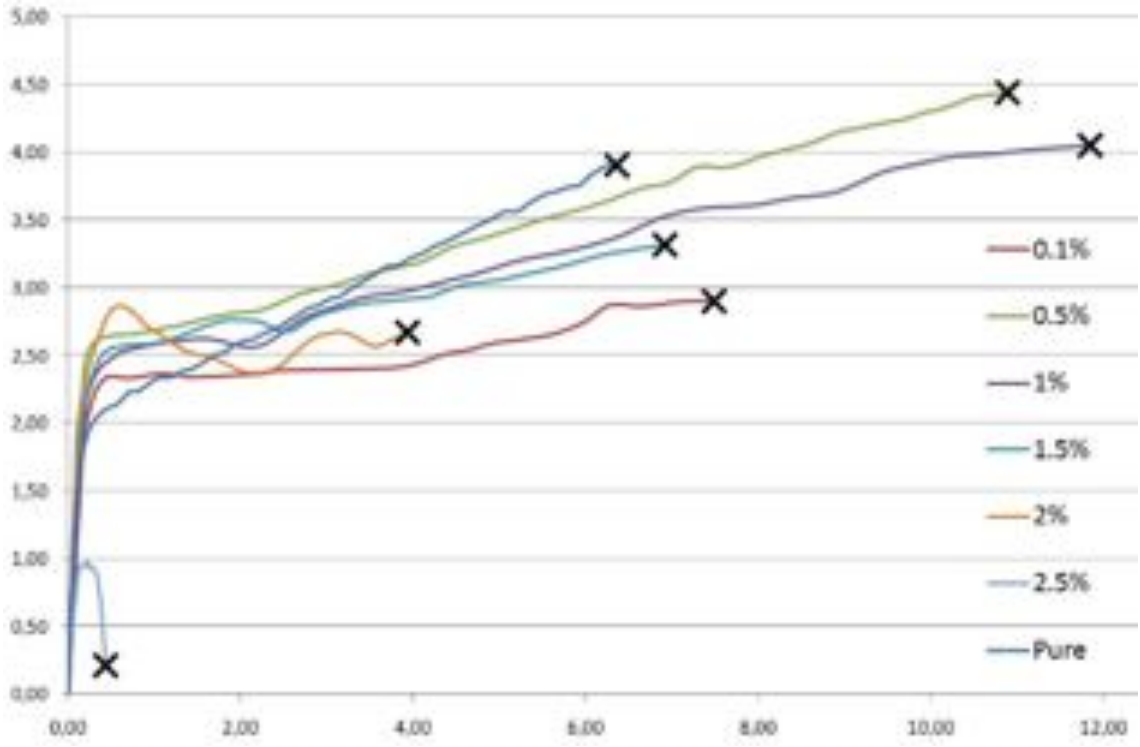

Figure 21: 2^{nd} protocol results, Engineering stress (MPa) / Engineering strain

Nevertheless, this reinforcement is dependent on the CNTs amount. Showing the optimal nanocomposite behavior, the array 4 and the figure 22 underline this amount effect. As presented in the literature review, several parameters influence

the nanocomposites. Besides the mechanical behavior of the reinforcement, the enhanced material behavior also depends on the nanoparticles dispersion [11, 15].

According to the results presented below, the optimal material seems to be the polyurea matrix reinforced with 0.5 wt% of CNTs. This enhancement proportion almost doubles the maximum strain while a 13% increase is noticed on ultimate stress.

Beyond the optimal CNT amount, the mechanical properties are degraded. Increasing the reinforcement quantity, the dispersion is worse. As the 1^{st} protocol results show, due to the CNT aggregates (equivalent to defects) in the material structures, the behavior is different from the expected one. The specimen with 2.5 wt% CNT added showed the worst behavior, as it broke almost immediately under small loads and small elongations, which is an indication of brittle-type behavior.

wt% CNTs	Maximum strain	Ultimate stress (MPa)
0	6.4	3.9
0.1	7.4	2.9
0.5	10.8	4.4
1	11.8	4.1
1.5	6.8	3.3
2	3.8	2.6
2.5	0.4	0.3

Table 4: CNT-based composite properties

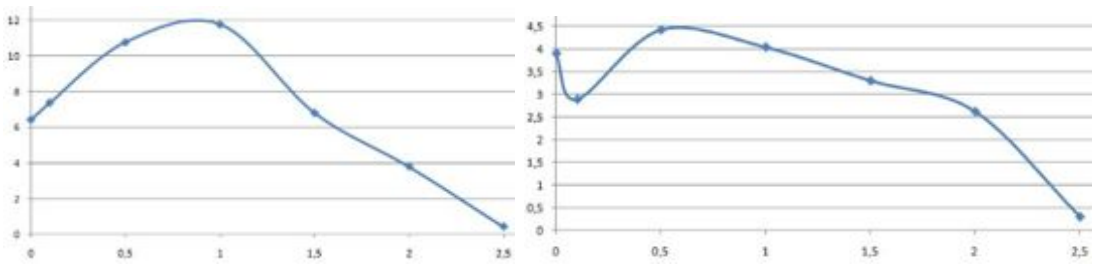

(a) (b)

Figure 22: 2^{nd} protocol results: (a) maximum strain / wt%(CNTs); (b) ultimate stress (MPa) / wt%(CNTs)

Fractographic analysis

The SEM picture in figure 23, shows the nanostructure of the cracking section (CNT nanocomposite optimum found above).

- First, the CNT dispersion seems better in this case than in the 1^{st} protocol. The SEM visualization on this type of material has not highlighted CNT aggregates with the same size as the previous nanocomposite. As shown in this picture, CNT network seems well dispersed; they are not assembled into packages.
- Second, the interaction reinforcement/matrix seems strong, as CNTs give the impression they are well coated by the polyurea matrix (good transition, between the free CNTs and the matrix without cavity at their roots). Furthermore, very few CNTs were actually observed, which suggest that the polymer matrix has thoroughly coated the nanoparticles, making strong bonds increasing the interface Polyurea/CNTs. At the same time, due to this good matrix adhesion, CNTs retard the crack propagation. Indeed, due to their impressive mechanical properties, CNTs with a vertical orientation relative to the plane of the crack limit the progress of it.

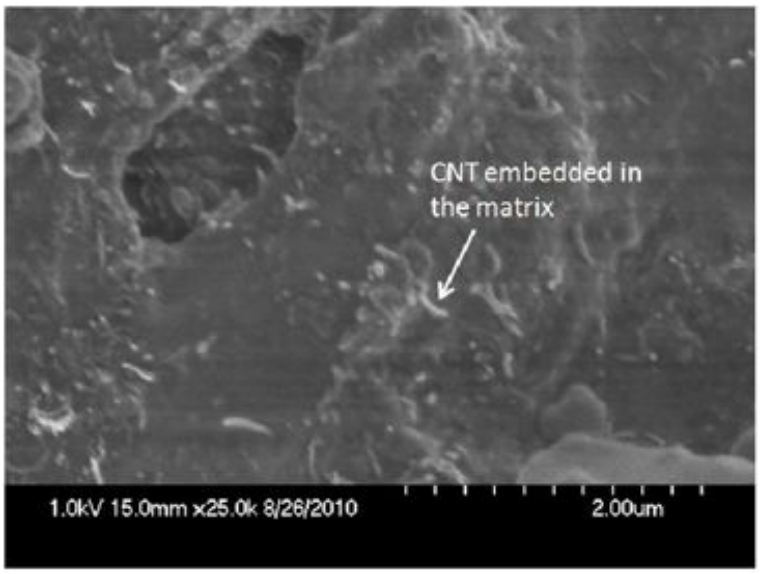

Figure 23: Nanocomposite (0.5 wt% of CNTs), interaction CNT/Matrix (Magnification x25000)

4.1.4 Second protocol results, GNP enhancement

Due to the current interest on the GNP as a matrix reinforcement, it was obvious to compare the behavior of the matrix with different enhancements. This subsection presents the experimental results using the 2^{nd} manufacturing protocol and GNPs as polyurea reinforcement.

Mechanical behavior

As previously shown, figure 24 observes the mechanical behavior for the GNP-

based nanocomposite. All the specimens show an initial linear behavior, with a high value of Young's modulus, up to a stress level that ranges between 2.0 - 2.7 MPa. Once this value is reached, the stress/strain behavior remains linear but with a slope that depends on the amount of GNPs used.

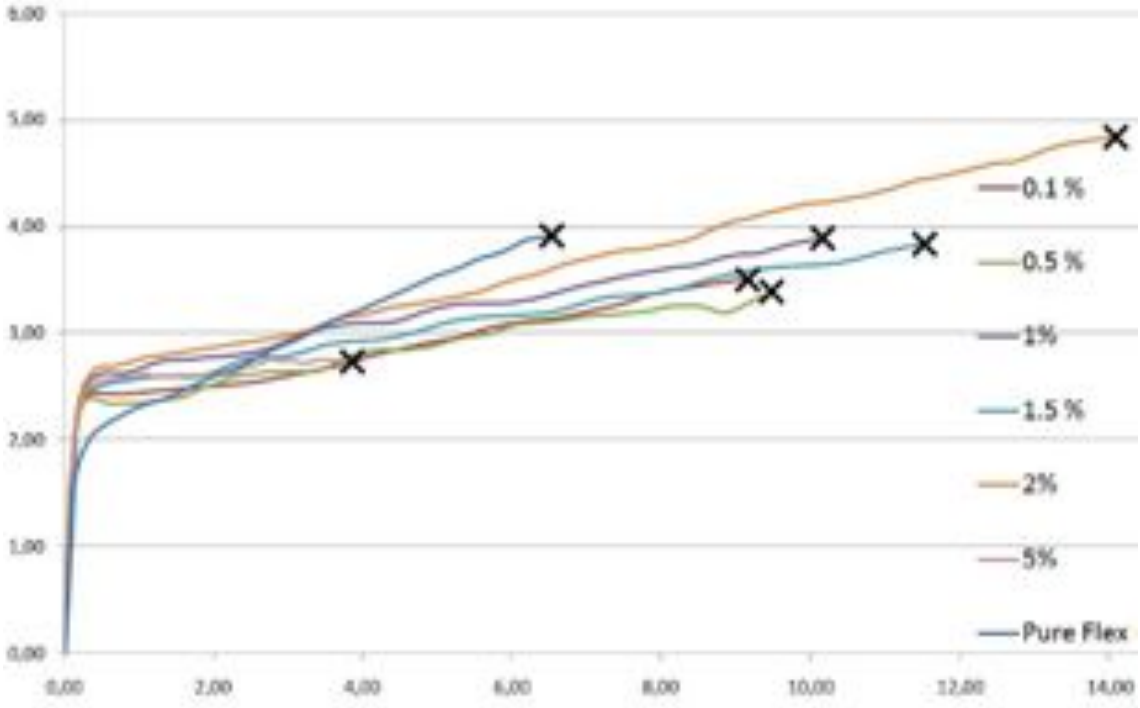

Figure 24: 2^{nd} protocol results, Engineering stress (MPa) / Engineering strain

As illustrated in the array 5 and figure 25, the addition of GNPs improves the tensile of some samples. Because of the improvement of the maximum strain and stress with the reinforcement amount, these curves portray the enhancement interest. The best performance is recorded for the sample with 2 wt% GNP doped-polyurea specimen. The final elongation reached was almost 1400%, which indicates an increase of more than two times greater than the commercial matrix (elongation of about 600%).

As previously shown, beyond the optimal GNP amount, the mechanical properties are degraded. The specimen with 5 wt% GNP added showed the worst behavior as it broke faster than the other reinforcement quantities under small loads and small elongations.

wt% GNPs	Maximum strain	Ultimate stress (MPa)
0	6.4	3.9
0.1	9.0	3.5
0.5	9.3	3.3
1	10.0	3.7
1.5	11.4	3.9
2	13.9	4.8
2.5	3.8	2.7

Table 5: GNP-based composite properties

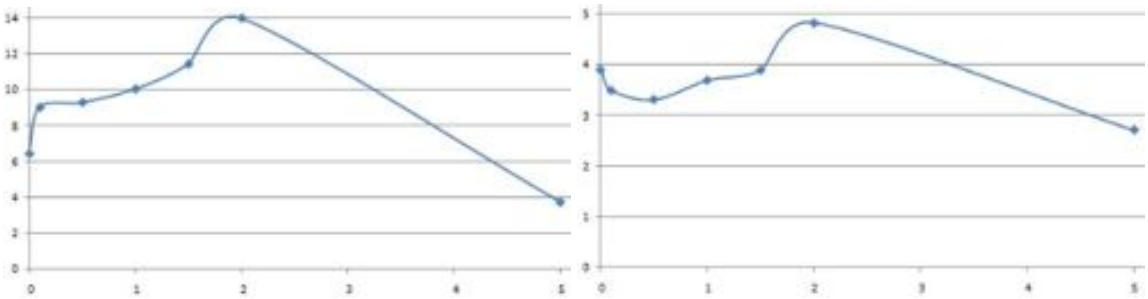

(a) (b)

Figure 25: 2^{nd} protocol results: (a) maximum strain / wt%(GNPs); (b) ultimate stress (MPa) / wt%(GNPs)

4.1.5 Optimal nanocomposite, amount and enhancement type

Comparing the both optimums found in the previous subsection, the GNP doped nanocomposite shows the best behavior. Figure 26 compares the stress/strain curves for the pure matrix with the CNT and GNP optimum nanocomposites. The GNP enhancement corresponds to a reinforcement almost twice that of CNT.

Due to the close behavior of these nanoparticles, the better behavior of the GNP nanocomposite could be explain by taking in consideration the shape of the reinforcements and their interaction with the matrix. Indeed, the load transfer between the matrix and the GNP is better because of the shape ratio of these nanoparticles comparing with that of the CNTs. i.e. the GNP/Matrix interaction surface is bigger than that of the CNT/Matrix.

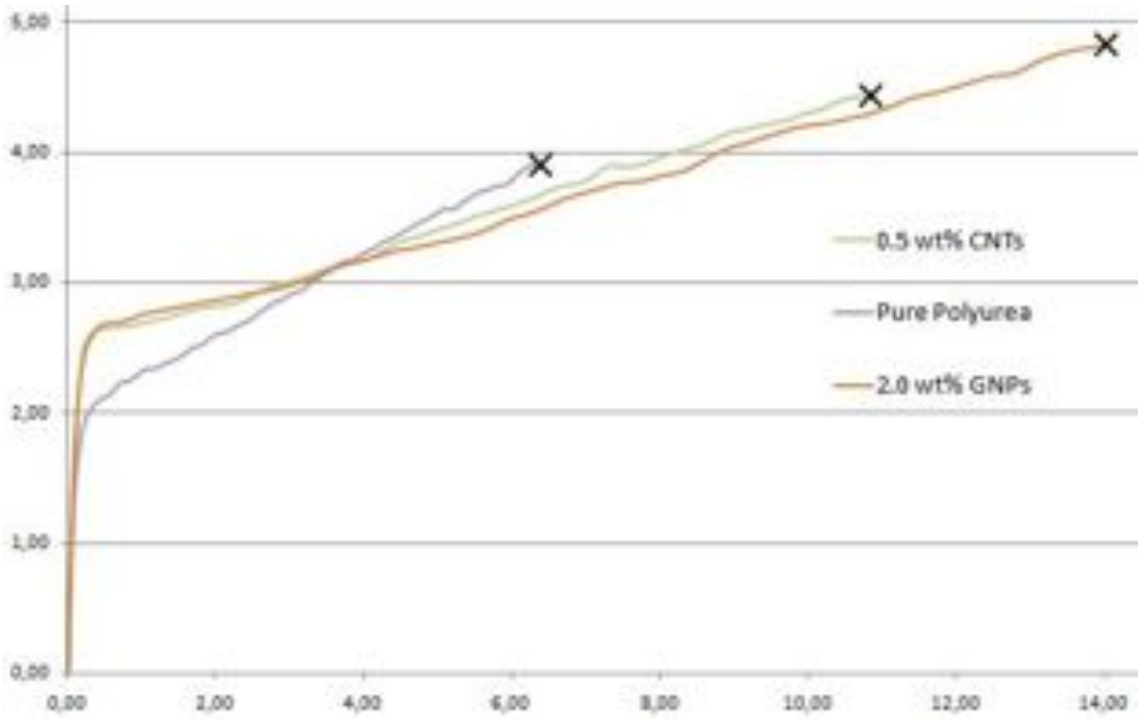

Figure 26: Comparison , Engineering stress (MPa) / Engineering strain

4.2 Finite elements model

This subsection presents the computational material modeling for both nanocomposites made by using the second protocol. At this stage of study, these results are not exhaustive. The aim is to introduce the main goal of the method. The material evaluation has been done for each enhancement amount in order to get a general model expressing a function of the model parameter with the reinforcement percentage.

4.2.1 MCalibration and Abaqus modeling

Using the modeling method presented above, two material models have been used to describe the mechanical behavior for the nanocomposites enhanced by CNT or GNP. The following paragraphs present quickly the theory and the optimization results relative to each model.

CNT nanocomposite modeling with the Ogden model

$$\begin{cases} \lambda_1 & = 1+\epsilon \\ \lambda_2 & = (1+\epsilon)^{-1/2} \\ U & = \sum_{i=1}^{N} \frac{2*\mu_i}{\alpha_i^2} \left(\lambda_1^{\alpha_i} + \lambda_2^{\alpha_i} + \lambda_1^{-\alpha_i}\lambda_2^{-\alpha_i} - 3\right) \\ \sigma & = \lambda_1 \frac{\partial U}{\partial \lambda_1} \end{cases} \tag{2}$$

Equation system 2 shows the Ogden model theory used in this material model. As presented in the method section, the hyperelastic model is based on the strain energy potential calculation in order to determine the behavior law of the material ($\sigma = f(\epsilon)$). N determines the order of the strain energy potential U. Used by MCalibration, this theory is able to describe the material behavior for a large scale of strain. The found parameters are presented in the array 6.

wt% CNTs	μ_1	α_1	D_1	μ_2	α_2	D_2
0	1.35	0.37	0.01	0.29	2.09	0.01
0.1	1.29	0.34	0.01	0.25	1.82	0.01
0.5	1.68	0.33	0.01	0.24	2.02	0.01
1	1.55	0.36	0.01	0.26	1.92	0.01
1.5	1.68	0.34	0.01	0.26	1.81	0.01
2	1.45	0.04	0.01	0.27	1.14	0.01

Table 6: Ogden parameters for the CNT nanocomposite modeling

GNP nanocomposite modeling with the Hyperfoam model

$$\begin{cases} \lambda_1 & = 1+\epsilon \\ \lambda_2 & = \lambda_3 = (1+\epsilon)^{-1/2} \\ U & = \sum_{i=1}^{N} \frac{2*\mu_i}{\alpha_i^2} \left(\lambda_1^{\alpha_i} + \lambda_2^{\alpha_i} + \lambda_3^{\alpha_i} - 3 + \frac{1}{\beta_i} * (J^{-\alpha_i * \beta_i} - 1) \right) \\ \sigma & = \lambda_1 \frac{\partial U}{\partial \lambda_1} \end{cases} \tag{3}$$

Equation system 3 is based on the same meaning as system 2. The parameters for this material model are highlighted in table 7.

wt% GNPs	μ_1	α_1	β_1	μ_2	α_2	β_2
0	0.12	2.55	0.20	2.07	0.45	0.20
0.1	0.08	2.46	0.20	2.32	0.35	0.20
0.5	0.10	2.25	0.20	2.09	0.47	0.20
1	0.08	2.36	0.20	2.32	0.48	0.20
1.5	0.10	2.27	0.20	2.30	0.41	0.20
2	0.09	2.41	0.20	2.87	0.31	0.20
5	0.06	2.24	0.20	2.81	0.16	0.20

Table 7: Hyperfoam parameters for the GNP nanocomposite modeling

4.2.2 Model generalization

CNT nanocomposite

In order to get a general model, an interpolation is needed to get a general function for each parameter of the model depending on the enhancement amount in the polyurea matrix. The aim goal being to predict the mechanical behavior of the nanocomposite by knowing the enhancement amount.

This interpolation had been proceeded using the interpolation toolbox in Matlab. Figure 27 shows the interpolation results, as related in the beginning of this section, these results are not exhaustive. In fact, due to the number of the points the interpolation is not accurate. A suitable model could be obtained with more experimental data from more sample compositions.

Although the results are not precise, they show the way to get a general material model definition for a complex material behavior. As presented in the modeling method section, because of the its nonlinearity, an hyperelastic material modeling is a tough task to achieve. Knowing the approximation of this method, it is a first step in the material modeling.

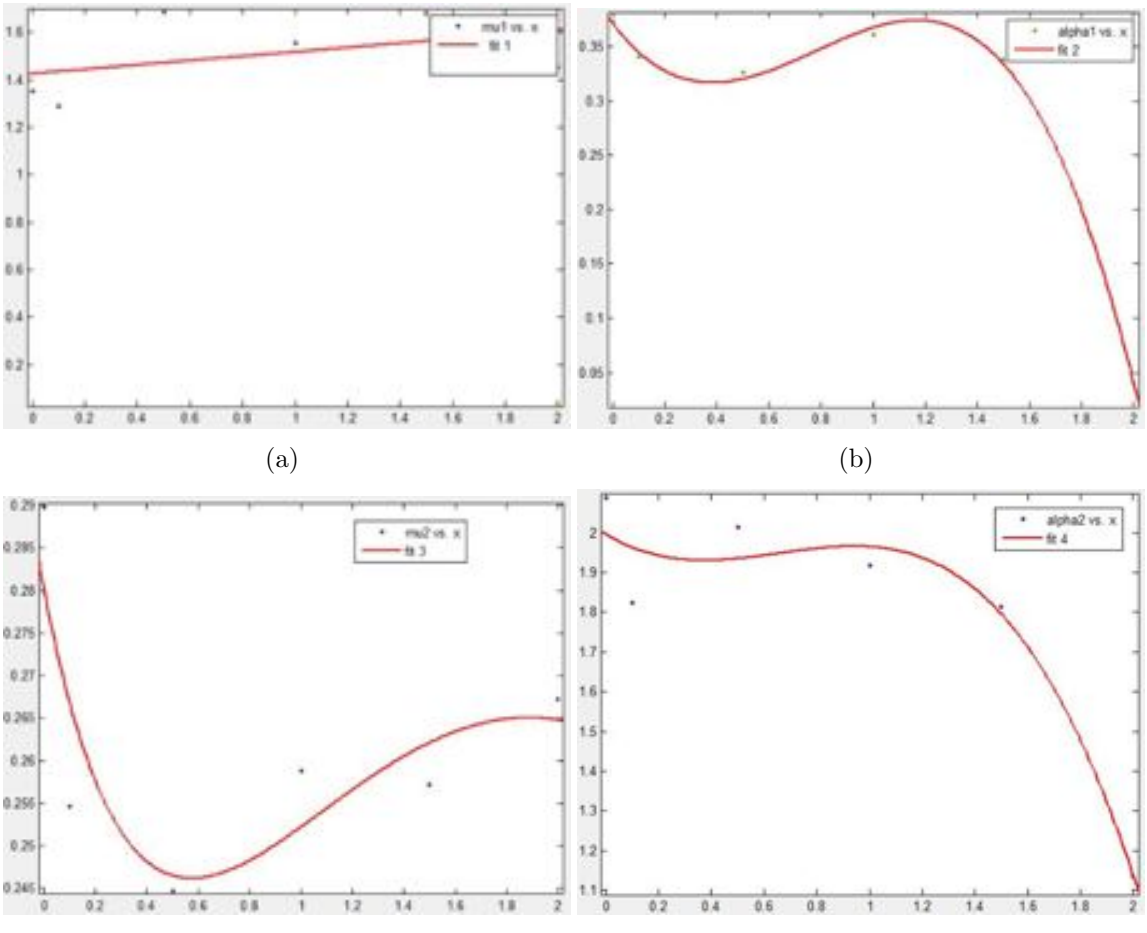

(a) (b)

(c) (d)

Figure 27: Ogden model parameters and interpolation (parameter value / wt%(CNTs)): (a) Mu1; (b) Alpha1; (c) Mu2; (d) Alpha2

5 Conclusion

In this study we analysed the influence of CNTs and GNPs in Polyurea's mechanical behavior to evaluate the optimal amount of each nanoparticles that yields the best overall mechanical performance.

Comparing the results presented above, the nanoparticles dispersion is the main parameter in the Polyurea enhancement. Without a doubt, the ultrasonic stirring is the most suitable way to brake the aggregates in order to get a homogenous nanoparticles solution. Hence, our first conclusion is that the manufacturing protocol is a key point on the nanomaterial enhancement expectation.

Working on the best suitable manufacturing protocol, we dispersed different quantities of CNTs and GNPs into the Polyurea matrix to obtain different nanocomposites with varying mechanical behavior. These tests show that the mechanical performance of Polyurea can be significantly enhanced by adding a certain amount of nanoparticles. While we observed substantial enhancement when only 0.5 wt% CNTs or 2 wt% GNPs were added. Adding other quantities gave much weaker performance in terms of ultimate strength and elongation. Furthermore, comparing these nanocomposite optimums, the GNP doped-material showed a better behavior with a maximum strain and stress. The GNP enhancement corresponded to a reinforcement twice that of CNT. Hence, our second conclusion is that the amount and the type of reinforcement should be carefully chosen to get a nanocomposite with the expected behavior.

Despite the conclusion presented above, due to the time allotted for this research, the temperature effect, the aging impact and the tribology study[27] was not studied. These important parameters are required to conclude on material behavior on the spot. In order to finalize this study and to get an appropriate conclusion related to the application, Luciana Balsamo, a PhD student at Columbia University will continue this research project during her thesis. This thesis will be also provide the opportunity to use and develop the hyperelastic model to find a more suitable evaluation, taking into account the effects introduced above.

[27] interaction between the nanocomposite layer and the cable

References

[1] T. Asami and K-H. Nitta. Morphology and mechanical properties of polyolefinic thermoplastic elastomer i. characterization of deformation process. *Polymer*, 45:5301–5306, 2004.

[2] J. Bergstrom. *J. PolyUMod, a library of user materials for ABAQUS*. Veryst Engineering, LLC, 2010.

[3] J. Bergstrom. *MCalibration manual*. Veryst Engineering, LLC, 2010.

[4] Y. Geng, S. J. Wang, and J-K Kim. Preparation of graphite nanoplatelets and graphene sheets. *Journal of Colloid and Interface Science*, 336:592–598, 2009.

[5] Y.H. Ho, C.P. Chang, F.L. Shyu, R.B. Chen, S.C. Chen, and M.F. Lin. Electronic and optical properties of double-walled armchair carbon nanotubes. *Elsevier, Carbon*, 42:3159–3167, 2004.

[6] S. Iijima. Carbon nanotubes: past, present, and future. *Physica B*, 323:1–5, 2002.

[7] ASTM International. Standard test methods for vulcanized rubber and thermoplastic elastomers-tension. *ASTM International*, D412-06a:1–14, 2010.

[8] T. Kuilla, S. Bhadra, D. Yao, N.H. Kim, S. Bose, and J.H. Lee. Recent advances in graphene based polymer composites. *Progress in polymer science*, Accepted Manuscrit, 2010.

[9] M. Kulkarni, D. Carnahan, K. Kulkarni, D. Qian, and J. L.Abot. Elastic response of a carbon nanotube fiber renforced polymeric composite : a numerical and experimental study. *Elsevier*, B 41:414–421, 2009.

[10] V. Likodimos, S. Glenis, and L. Lin. Electronic properties of boron-doped multiwall carbon nanotubes studied by esr and static magnetization. *Physical review*, B 72:045436(1–7), 2005.

[11] P.C. Ma, N.A. Siddiqui, G. Marom, and J.K. Kim. Dispersion and functionalization of carbon nanotubes for polymer-based nanocomposites. *Composites Part A: Applied Science and Manufacturing*, In Press, Corrected Proof, 2010.

[12] George R. *International Journal of Critical Infrastructure Protection*, 2008.

[13] C.M. Roland, J.N. Twigg, Y. Vu, and P.H. Mott. High strain rate mechanical behavior of polyurea. *Elsevier, Polymer*, 48:574–578, 2006.

[14] J.P. Salvetat, J.M. Bonard, N.H. Thomson, A.J. Kulik, L. Forro, W. Benoit, and L. Zuppiroli. Mechanical properties of carbon nanotubes. *Applied Physics A, Materials Science and Processing*, 69:255–260, 1999.

[15] XG Sciences. *Dispersion notes*.

[16] Simula. *Abaqus user's manual*. Dassault Systemes, 2010.

[17] R. S.Ruoff, D. Qian, and W. Kam Liu. Mechanical properties of carbon nanotubes : theoretical predictions and experimental measurement. *C. R. Physique*, 4:993–1008, 2003.

[18] Technische fakultat der christian albrechts universitat, Kiel. *Test M604: Scanning electron microscopy*.

[19] H.D. Wagner and R.A. Vaia. Nanocomposites : issues at the interface. *Materials today*, 7:38–42, 2004.

[20] M-K. Yeh, T-H. Hsieh, and N-H. Tai. Fabrication and mechanical properties of multi-walled carbon nanotubes/epoxy nanocomposites. *Elsevier, Material science and engineering A*, 483-484:289–292, 2006.

6 Appendix

6.1 Which solvent for the nanoparticles dispersion

There is still a long road to create nanoparticle reinforcement composites, fully realizing the potential of high strength and stiffness of the CNTs or the GNPs. There are many reasons for this limitation. As presented in the method section, the nanoparticles dispersion is the main point in the nanocomposite manufacturing. This appendix investigates this effect and presents the way to reduce its influence in the nanocomposite behavior. This study presents the best method to disperse the CNTs (the GNPs dispersion is equivalent).

The CNTs dispersion

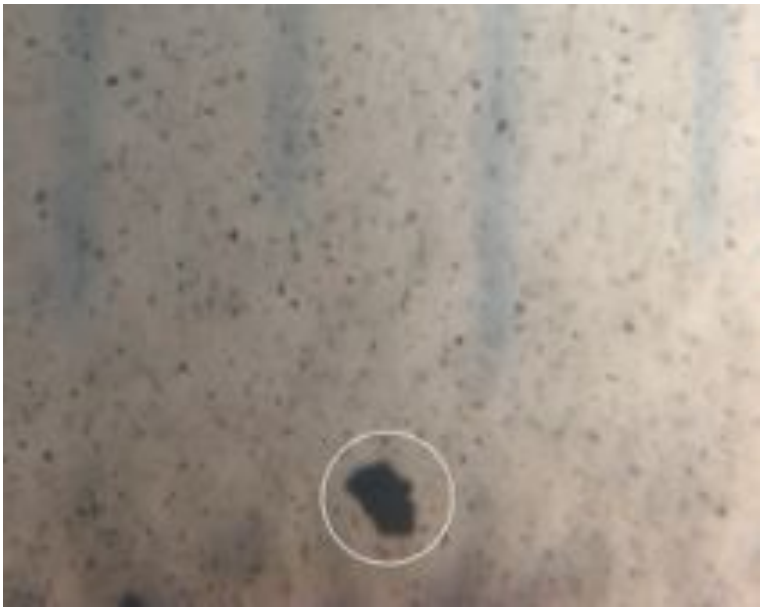

Figure 28: Photo of CNTs mechanically stirred in a solvent (THF)

Figure 28 shows the nanoparticles in the solvent after a mechanical stirring. These particles are visible with the naked eye (agglomerates in a solvent, see the circle in figure 28). The problem is that the nanocomposite needs a homogeneous enhancement in the matrix, to make the dispersion more homogeneous. To get a better solution, an ultrasonic stirring, using the probe sonicator in Figure 29 (a), was performed. With the same CNT amount and the same solvent, Figure 29 (b) shows the difference between a mechanical and an ultrasonic stirring. Obviously, the ultrasonic stirring is more efficient than the mechanically stirred solution. The black solution indicates a good CNT dispersion.

Solvent evaluation

A solvent evaluation was done to specify which available solvent is the most convenient for the CNT dispersion. In this section, CNTs were dispersed in 3 different

(a) (b)

Figure 29: (a) Ultrasonic stirring by using a Sonicator *hielscher UP50H*; (b) Comparison of stirring methods : Ultrasonic (left) / Mechanical stirring (right)

solvents which are : Tetrahydrofuran, Ethanol and Distilled water. The dispersion was performed using the previous protocol (1 hour of ultrasonic stirring). The amount of CNTs and the solvent volume were exactly the same for each solution.

After stirring, the solution is filtered. In fact, due to the high amount of CNTs and their quality (90 % pure), the stirring is actually not exactly done for all the nanoparticles. The using of a centrifuge (figure 31 on page 52) is used to filter the solution and to distinguish the dispersed CNTs to the CNT agglomerates and the other carbon particles (graphite for example). The solution was filtered for 4 minutes at 5000 rpms, the upper part of the solution (3/4 of the solution) was then removed with a teated pipette to get only the CNTs dispersed in the solvent (CNTs are lighter than the other particles in the solution). The following figures present the results for several solvents.

Figure 32 on page 53 shows the CNT dispersion in the 3 studied solvents. In that study, 0.24 g of CNTs were dissolved in each solvent and then the solutions were stirred and filtered as previously. In that case, the darker the solution was, the more the CNTs were dispersed. In fact, a darker solution means a higher concentration in thin and light weight particles. This observation is more qualitative than quantitative. The aim is to compare the CNT's dispersion in several solvents.

Figure 33 shows the CNT dispersion in the THF and the distilled water. In that study, 0.024 g of CNTs were dissolved in each solvent and then the solutions were stirred and filtered as previously. This experience shows the role of the amount of CNT in the dispersion. The higher the CNT amount, the harder the dispersion

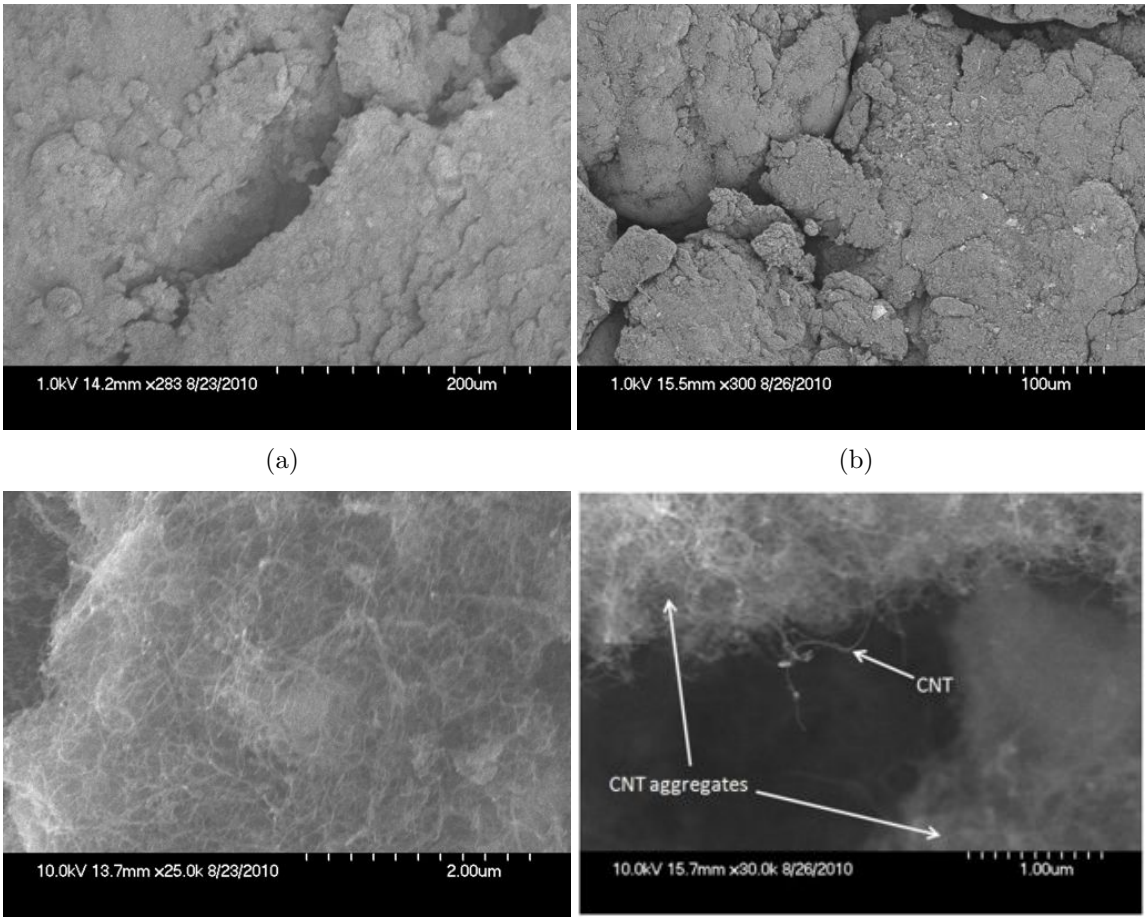

(a) (b)

(c) (d)

Figure 30: (a) Sonicated CNTs (Magnification x283); (b) Original CNTs (Magnification x300); (c) Sonicated CNTs (Magnification x2500); (d) Original CNTs (Magnification x30000)

(a) (b)

Figure 31: Centrifuge *Sorvall LEGEND X1*: filtration of the solutions to highlight the solvent effect in the CNTs dispersion

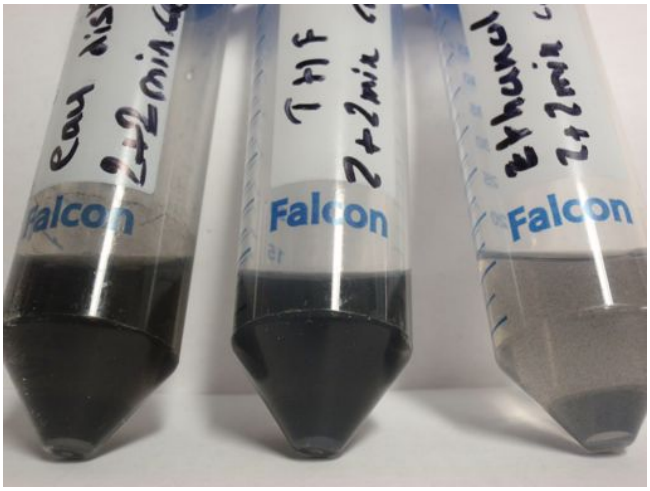

Figure 32: Solvent comparison after sonicator and centrifuge steps(0.34 g of CNTs in 40 ml of solvent) *From left to right : Distilled water, THF, Ethanol*

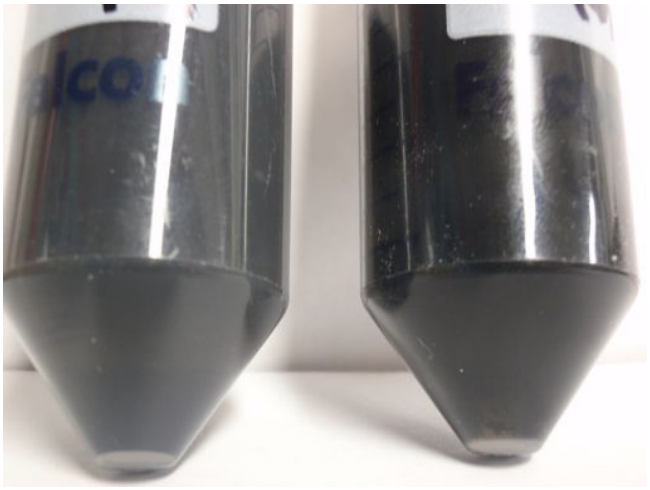

Figure 33: Solvent comparison after sonicator and centrifuge steps(34 mg of CNTs in 40 ml of solvent) *From left to right : THF, Distilled water*

is. In fact, after the stirring and the filtering, the solutions are still dark and the wastes (other particles) are almost not present in the solution. The second goal of this experience was to choose the best solvent for the CNT's dispersion and for the nanocomposite manufacturing.

As shown in the figure 33, the distilled water seems better than the THF (darker solution). In this way we tried to manufacture the nanocomposite using the distilled water as solvent. Due to the hydrophobic property of the used resin, we were forced to use another solvent more suitable. The withheld solvent for the nanocomposite manufacturing was then the THF (figure 34). The second main point about the use of the THF instead of the distilled water was the boiling temperature (66 degrees Celsius for the THF and 100 degrees Celsius for the water). In fact, the solvent boiling step required a higher temperature for the water.

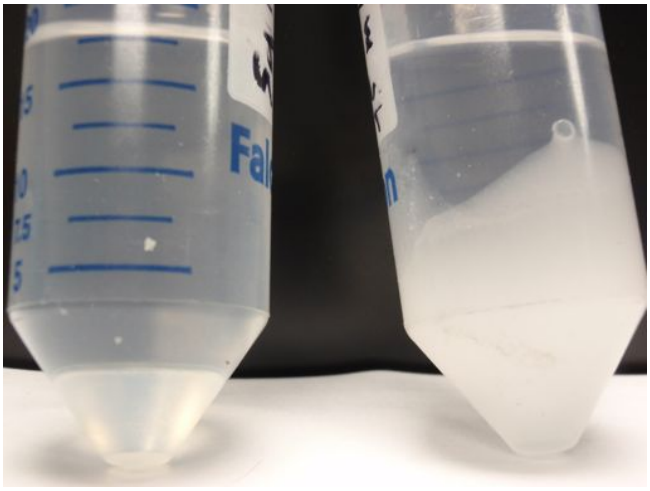

Figure 34: THF or distilled water in the matrix? *From left to right : THF, Distilled water*

6.2 Strain rate in the rubber materials

In the determination of the strain rate effect, MCalibration is a suitable software. Due to the time limits to perform this research, it has been difficult to practice different tests on the samples. Because of the viscous behavior of the model, where the deformation speed is taken in consideration, the best way was to evaluate the strain rate effect using the computational model.

The four graphics in Figure 35 highlight this effect. In this study, four strain rates were loaded in the virtual experiment determination in the MCalibration software. Comparing the experimental data (strain rate about 0.2 corresponding to a 2.0 inch/min deformation speed) with the predictions, conclusions on this effect have been made. Indeed, as shown in the figure 35, the faster the deformation, the stronger the material.

According to these results, a standard [7] strain rate is required to get comparable results in experimental studies.

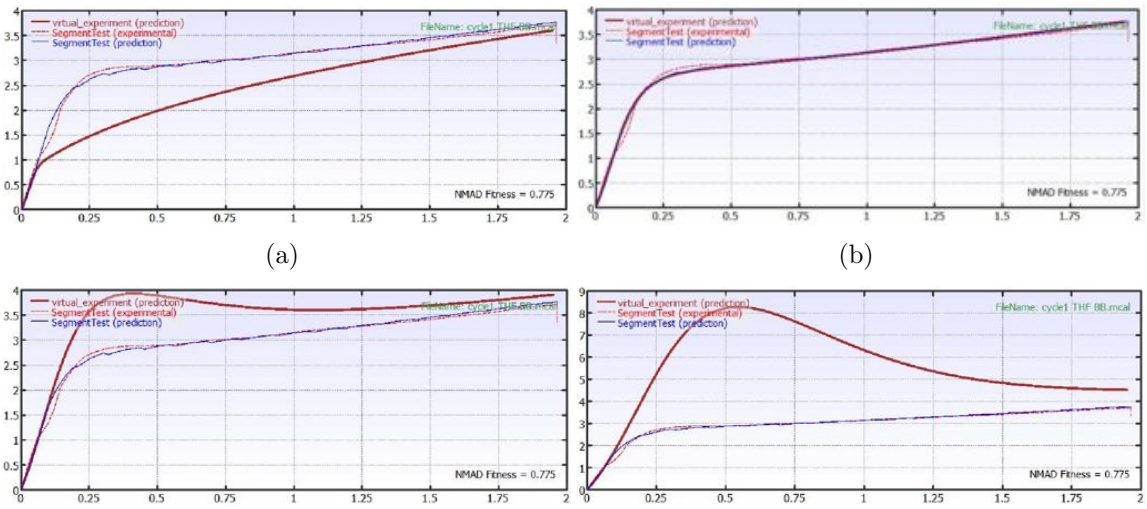

Figure 35: Behavior prediction, Engineering stress (MPa) / Engineering strain (a) Strain rate = 0.02 ; (b) Strain rate = 0.2; (c) Strain rate = 0.5; (d) Strain rate = 2

6.3 Interaction between MCalibration and Abaqus

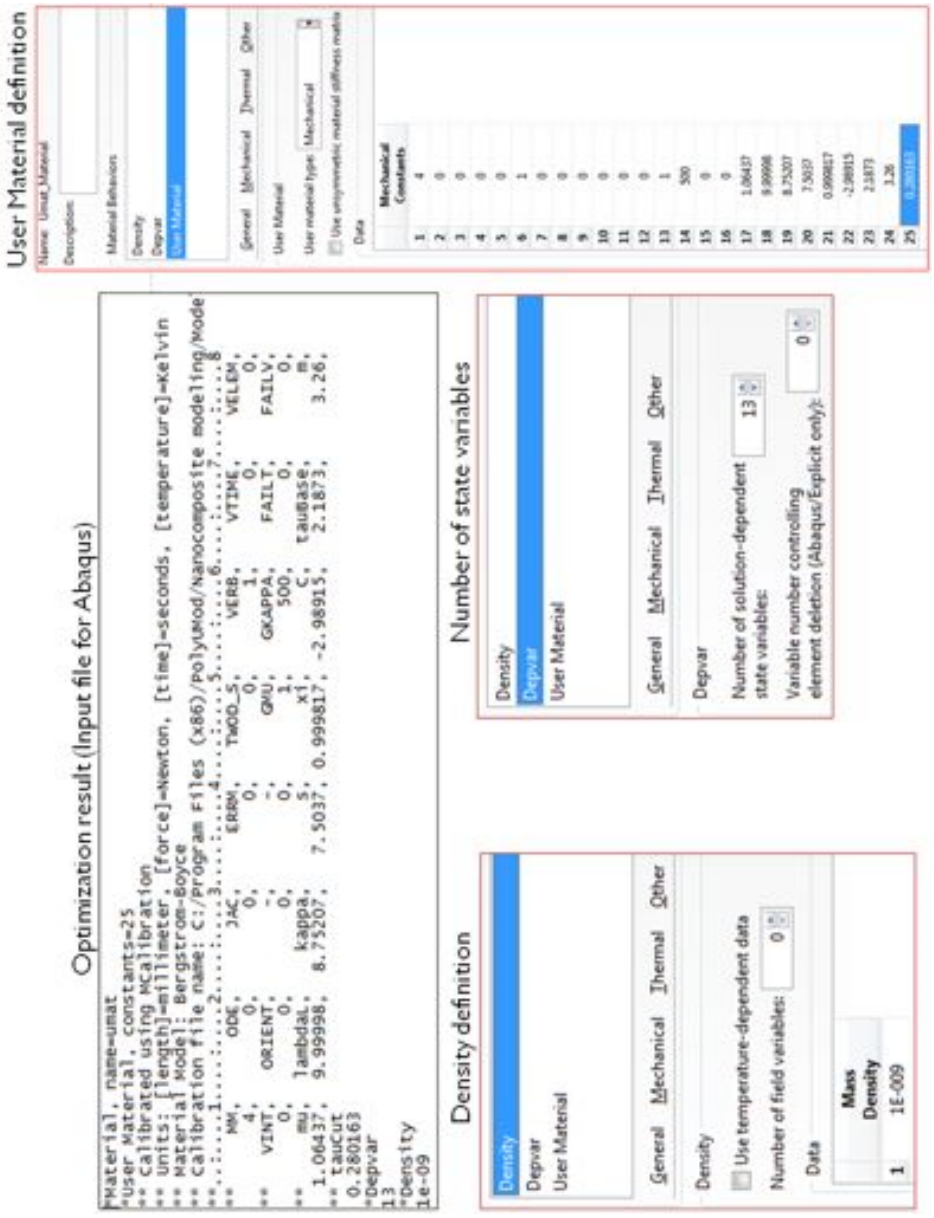

Figure 36: Modeling method using a MCalibration input file

6.4 Matlab smoothing program

```
%%%%%%%%%%%%%%%%%%%%%%%%%%%%%%%%%%%%%%%%%%%%%%%%%%%%%%%%%%%%%%%%%%%%%%%%%%%%
%%%%%%%%%%%           Carbon NanoTubes Enhancement              %%%%%%%%%%%
%%%%%%%%%%%%%%%%%%%%%%%%%%%%%%%%%%%%%%%%%%%%%%%%%%%%%%%%%%%%%%%%%%%%%%%%%%%%

clc
clear all

% 1 --> 0.1% CNTs
% 2 --> 0.5% CNTs
% 3 --> 1.0% CNTs
% 4 --> 1.5% CNTs
% 5 --> 2.0% CNTs
% 6 --> 2.5% CNTs
% 7 --> 0.0% (PURE)

load yCNT.txt
load xCNT.txt

x = xCNT;
y = yCNT;

x1 = find(x(:,1));
x1 = x(x1,1);
x2 = find(x(:,2));
x2 = x(x2,2);
x3 = find(x(:,3));
x3 = x(x3,3);
x4 = find(x(:,4));
x4 = x(x4,4);
x5 = find(x(:,5));
x5 = x(x5,5);
x6 = find(x(:,6));
x6 = x(x6,6);
x7 = find(x(:,7));
x7 = x(x7,7);

y1 = find(y(:,1));
y1 = y(y1,1);
y2 = find(y(:,2));
y2 = y(y2,2);
y3 = find(y(:,3));
y3 = y(y3,3);
y4 = find(y(:,4));
y4 = y(y4,4);
y5 = find(y(:,5));
y5 = y(y5,5);
y6 = find(y(:,6));
y6 = y(y6,6);
y7 = find(y(:,7));
y7 = y(y7,7);

sy1 = smooth(x1,y1,0.15,'rloess');
[xx1,ind] = sort(x1);
figure(1)
subplot(2,1,1)
plot(xx1,y1(ind),'b.',xx1,sy1(ind),'r-')
```

```
title('Smoothed Diagrqm for 0.1% CNTs Concentration','FontSize',20)
legend('Original Data','Smoothed Data','Location','NW')
subplot(2,1,2)
plot(xx1,sy1(ind),'r-')

sy2 = smooth(x2,y2,0.08,'rloess');
[xx2,ind] = sort(x2);
figure(2)
subplot(2,1,1)
plot(xx2,y2(ind),'b.',xx2,sy2(ind),'r-')
title('Smoothed Diagrqm for 0.5% CNTs Concentration','FontSize',20)
legend('Original Data','Smoothed Data','Location','NW')
subplot(2,1,2)
plot(xx2,sy2(ind),'r-')

sy3 = smooth(x3,y3,0.08,'lowess');
[xx3,ind] = sort(x3);
figure(3)
subplot(2,1,1)
plot(xx3,y3(ind),'b.',xx3,sy3(ind),'r-')
title('Smoothed Diagrqm for 1% CNTs Concentration','FontSize',20)
legend('Original Data','Smoothed Data','Location','NW')
subplot(2,1,2)
plot(xx3,sy3(ind),'r-')

sy4 = smooth(x4,y4,0.09,'lowess');
[xx4,ind] = sort(x4);
figure(4)
subplot(2,1,1)
plot(xx4,y4(ind),'b.',xx4,sy4(ind),'r-')
title('Smoothed Diagrqm for 1.5% CNTs Concentration','FontSize',20)
legend('Original Data','Smoothed Data','Location','NW')
subplot(2,1,2)
plot(xx4,sy4(ind),'r-')

sy5 = smooth(x5,y5,0.15,'lowess');
[xx5,ind] = sort(x5);
figure(5)
subplot(2,1,1)
plot(xx5,y5(ind),'b.',xx5,sy5(ind),'r-')
title('Smoothed Diagrqm for 2% CNTs Concentration','FontSize',20)
legend('Original Data','Smoothed Data','Location','NW')
subplot(2,1,2)
plot(xx5,sy5(ind),'r-')

sy6 = smooth(x6,y6,0.05,'rloess');
[xx6,ind] = sort(x6);
figure(6)
subplot(2,1,1)
plot(xx6,y6(ind),'b.',xx6,sy6(ind),'r-')
title('Smoothed Diagrqm for 2.5% CNTs Concentration','FontSize',20)
legend('Original Data','Smoothed Data','Location','NW')
subplot(2,1,2)
plot(xx6,sy6(ind),'r-')

sy7 = smooth(x7,y7,0.05,'rloess');
```

```
[xx7,ind] = sort(x7);
figure(7)
subplot(2,1,1)
plot(xx7,y7(ind),'b.',xx7,sy7(ind),'r-')
title('Smoothed Diagrqm for 0% CNTs Concentration','FontSize',20)
legend('Original Data','Smoothed Data','Location','NW')
subplot(2,1,2)
plot(xx7,sy7(ind),'r-')

sy1CNT=sy1; sy2CNT=sy2; sy3CNT=sy3; sy4CNT=sy4; sy5CNT=sy5; sy6CNT=sy6;
sy7CNT=sy7;
xx1CNT=xx1; xx2CNT=xx2; xx3CNT=xx3; xx4CNT=xx4; xx5CNT=xx5; xx6CNT=xx6;
xx7CNT=sy7;

save sy1CNT sy2CNT sy3CNT sy4CNT sy5CNT sy6CNT sy7CNT
save xx1CNT xx2CNT xx3CNT xx4CNT xx5CNT xx6CNT xx7CNT
```